Research Square

Preprints are preliminary reports that have not undergone peer review.
They should not be considered conclusive, used to inform clinical practice,
or referenced by the media as validated information.

Effects of chemical treatments on the swelling behaviour of clay-bearing geomaterials

Wanqi Zhang
University of New South Wales
Chengguo Zhang
chengguo.zhang@unsw.edu.au
University of New South Wales
Honghao Chen
University of New South Wales
Joung Oh
University of New South Wales
Ismet Canbulat
University of New South Wales
Serkan Saydam
University of New South Wales

Research Article

Keywords: Clay minerals, Swelling mechanisms, Chemical treatment, Spraying, Wetting and drying cycles, Floor heave.

Posted Date: November 6th, 2026

DOI: https://doi.org/10.21203/rs.3.rs-11407185/v1

License: This work is licensed under a Creative Commons Attribution 4.0 International License.
Read Full License

Additional Declarations: No competing interests reported.

Title

Effects of chemical treatments on the swelling behaviour of clay-bearing geomaterials

Authors

Wanqi Zhang, Chengguo Zhang*, Honghao Chen, Joung Oh, Ismet Canbulat, Serkan Saydam.

School of Minerals and Energy Resources Engineering, University of New South Wales, Sydney, Australia.

** Corresponding author: E-mail: chengguo.zhang@unsw.edu.au*

Abstract

Clay swelling causes volumetric expansion and compromises the stability of underground excavations. Chemical treatment serves as an essential approach for swelling control by affecting osmotic and intra-crystalline swelling mechanisms. This study assesses the swelling behaviour of compacted clays and intact rocks subjected to chloride salt solutions. Compacted clay specimens soaked in concentrated and dilute saline solutions behave differently due to the interplay between osmotic pressure and cation exchange reactions. At 1 mol/L, potassium chloride (KCl) more efficiently reduces clay swelling than sodium chloride (NaCl) and calcium chloride ($CaCl_2$), whereas at 0.1 mol/L, all salts slightly increase swelling deformation due to enhanced osmotic swelling. Spraying KCl is applied as a treatment step during wetting and drying cycles. Experimental results show that KCl-treated clays develop fewer surface cracks and exhibit reduced water retention during re-saturation, accounting for the limited expansion. KCl solution is also used to stabilise rock swelling and to provide a comparison with deionised water. The swelling potential of the rock is constrained by its strengthened rock matrix and further suppressed by the KCl treatment. Microscopic analyses are conducted on dry-state and post-treatment rocks. Both deionised water and salt solutions alter the surface morphology, as quantified by surface roughness parameters. KCl crystals are identified in high-contrast regions of microscopic images, while some crystalline phases may precipitate due to water evaporation. Enhancement of rock durability and assessment of groundwater chemistry are addressed to implement chemical treatment under field conditions, offering insights into optimising swelling control measures.

Keywords

Clay minerals; Swelling mechanisms; Chemical treatment; Spraying; Wetting and drying cycles; Floor heave.

Acknowledgement

The authors acknowledge Mark Whelan, Kanchana Gamage, and Kunze Li from UNSW Sydney for their assistance in laboratory testing. The authors thank the facilities and the scientific and technical assistance of Microscopy Australia at the Electron Microscope Unit (EMU) within the Mark Wainwright Analytical Centre (MWAC) at UNSW Sydney.

Highlights

- KCl (1 mol/L) exhibits enhanced swelling mitigation in compacted clays compared to NaCl and $CaCl_2$.
- Spraying chemical solutions can control swelling and reduce surface cracking during re-saturation.
- KCl reduces rock swelling and improves its durability against slaking and weathering.

1. Introduction

The swelling behaviour of clays in geological materials compromises the integrity of underground structures and leads to instability in engineering excavations. The observed volumetric expansion of clays and rocks arises from the physicochemical reactions between clay minerals and moisture from the environment. Numerous studies have been conducted to assess the influence of swelling clays in underground excavations (Bilir and Sarıgül 2021; Chen et al. 2025; Rastegarnia et al. 2021; Zhang et al. 2026). In some cases, swelling is intensified in areas of water accumulation, such as roadway floors, progressively softening the surrounding geomaterials and causing floor heave in the opening. For example, an inspection of a mine site in Newcastle coalfield reveals that soft claystone beds with abundant clays are gradually degraded by moisture and heaved up, nearly blocking the roadway (Galvin et al. 1999). Such swelling-induced instability emphasises the significance of research on swelling mechanisms and the development of control measures.

Multi-scale research was conducted to assess swelling properties of clay minerals and enhance the understanding of swelling mechanisms (Alaoui et al. 2025; Li et al. 2023). Laboratory tests are widely adopted to evaluate free swelling and confined swelling behaviour in an oedometer under different external loads (Guan et al. 2024; Pimentel 2015; Wang et al. 2023). Compared to laboratory tests, the measurement of in-situ swelling pressure can be affected by the precipitations formed during swelling (Steiner and Schwalt 2019). Moreover, sample preparation procedure causes additional disturbance and triggers water absorption before the measurement, underestimating the potential of swelling pressure (Zhang et al. 2020). Groundwater chemistry also influence the swelling evolution of clays in various geological settings (David 2018; Shehata et al. 2021).

Conventional control measures, such as drainage and floor dinting, primarily address volumetric swelling through mechanical methods. However, these methods typically provide a rapid but temporary way to maintain roadway clearance (Ghorbani et al. 2020; Mo et al. 2020; Nemcik 2003). In comparison, chemical treatment shows distinct advantages over mechanical methods by targeting swelling mechanisms. The core concept of chemical treatment lies in its effects on osmotic swelling and intra-crystalline swelling of clay minerals. Osmotic swelling is described by the Electrical Double-Layer theory, in which the repulsive force between diffuse double layers is intimately related to the Cation Exchange Capacity (CEC) of clay minerals (Madsen and Müller-Vonmoos 1989; Sridharan and Jayadeva 1982). Adding chemicals offers more exchangeable cations and facilitates cation exchange reactions. When cations from the added chemical, such as K^+, replace the original cations within the clay platelets and alter their CEC, osmotic water inflow is hindered, and swelling deformation is suppressed (Barakat et al. 2024; Xiang et al. 2020). Ion-exchange reactions have also been found to impede the intra-crystalline swelling, causing the deformation of rocks or compacted clays to be less detrimental and more manageable (Alzamel et al. 2022; Liu et al. 2018).

Chemical treatment should also minimise potential hazards to operational environment and production activities, such as chloride corrosion and sulphate contamination (Butscher et al. 2016; Hosseinzadeh et al. 2022). Extensive studies have been conducted to characterise the physico-chemical behaviour of swelling clays or rocks when subjected to various external loads and salt solutions in different concentrations, such as Opalinus Clay (Altmann et al. 2012; Barakat et al. 2024) and GMZ bentonite (Liu et al. 2018; Ma et al. 2024). Nevertheless, in the mining context, it is still challenging to predict swelling under saline or alkaline effects and develop associated control

measures. In particular, the drying and wetting cycles affects the swelling responses of rocks (Pejon and Zuquette 2002; Yang et al. 2019). Therefore, it is crucial to involve cyclic drying-wetting and explore its impacts on the effectiveness of chemical treatment.

This study investigates the swelling behaviour of compacted clay specimens and intact rock specimens under the influence of chemical solutions. The effects of cation type and concentration are evaluated through swelling tests on compacted clay specimens, followed by spraying KCl during wetting-drying cycles. KCl solution is then used in swelling tests on intact rock specimens. Microscopic analyses are applied for detailed characterisation of dry-state and post-treatment rocks, providing interpretations for the macroscopic observations in swelling tests. The findings demonstrate the effectiveness of chemical treatment and provide insights for floor heave assessment in swelling rocks.

2. Research workflow

Fig. 1 shows the research workflow of this study. Experimental materials, including raw clay materials and rock samples, are characterised with quantitative mineralogical analyses. Two types of specimens, compacted clay specimens and intact rock specimens, are prepared for swelling tests. Compacted clay specimens are reconstituted materials that represents a comparable mineral composition to that of rock samples collected from the field. Sample preparation procedures are detailed in the workflow, and both types of specimens are oven-dried before swelling tests. The effects of chloride salt solutions are evaluated against deionised water, considering cation type and cation concentration. The selection of the salt solution for enhanced swelling mitigation is based on the results obtained from compacted clay specimens. The influence of spraying KCl is further assessed during wetting-drying cycles. KCl solution is also used in swelling tests on intact rock specimens. Scanning electron microscopy (SEM) and energy-dispersive X-ray spectroscopy (EDS) are employed to examine microscopic changes in the post-treatment rock specimens. Additional practical considerations for chemical treatment are also discussed.

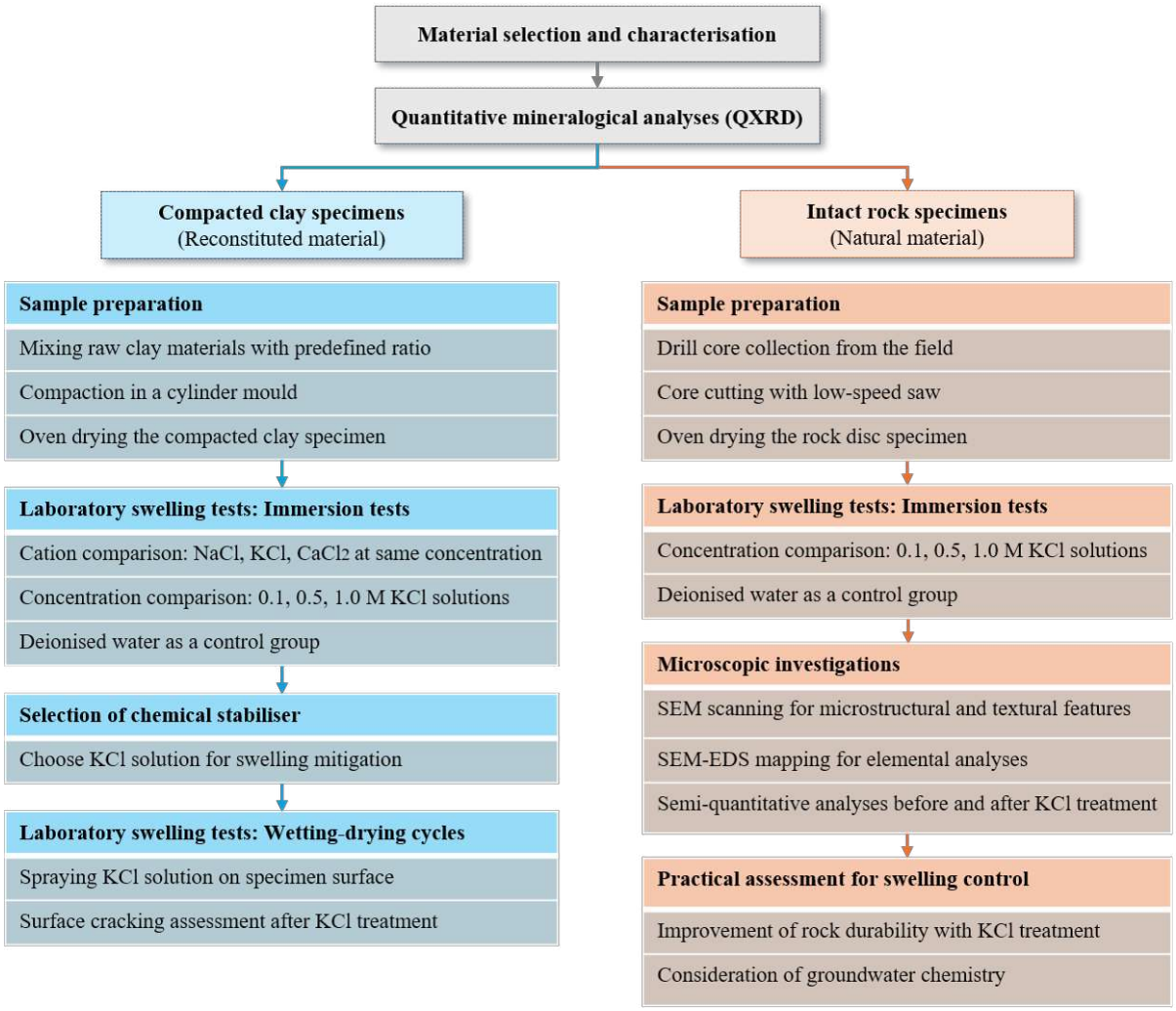


Fig. 1 Research workflow of this study.

3. Material and methods

3.1 Sample preparation

3.1.1 Intact rock specimens

Previous studies have documented swelling-induced roof and floor instabilities in the Newcastle Coalfield, New South Wales, Australia (Hebblewhite et al. 2005; McNally and Branagan 2014; Seedsman 1988). The floor strata, mainly consisting of claystone, are relatively competent in dry conditions but progressively soften when exposed to water, i.e., causing volumetric expansion. Hence, cores are drilled from a mine site in the Newcastle Coalfield to capture the swelling properties of claystone and assess swelling-induced instability in the same study area. Drill cores are wrapped and stored in a sealed box to prevent breakage and moisture loss during delivery to the laboratory. After delivery, cores are stored in a humidity-controlled and temperature-controlled room.

Drill cores are collected from a depth of cover ranging from 342 to 376 m. Most cores display buff or grey colour, with sandy-phase grains present on the surface. Rock discs are obtained by saw cutting at low speed to achieve the desired dimensions. Rock discs have an average diameter of 60.6 mm and an average height of 25.5 mm. The dry density of the rock ranges from 2.05 to 2.20 g/cm^3, and the porosity ranges from 16.7% to 17.5%, according

to the ISRM suggested methods (ISRM 1979). Rock fragments are crushed and ground into finer powders for quantitative X-ray diffraction (QXRD) analyses. The detected limit for phase identification is 0.5% by weight. Mineralogical analyses of pulverised rocks aim to quantify the content of clay minerals, such as smectite, offering valuable information on the swelling potential of the tested material.

The accurate measurement depends on the consistency of specimens. Using intact rocks introduces uncertainty due to the internet heterogeneity of rock formations, leading to inevitable discrepancies. Evidence suggests that the content of montmorillonite can vary from 10% to 30% of the floor, which points to the expansive tendency of the claystone floor in moisture conditions (Vasundhara 1999). Another concern is that some rocks are highly reactive to water and may collapse suddenly, introducing additional uncertainty into the measurement. In contrast, compacted clays are less affected by mineralogical heterogeneity, allowing for a more reliable testing procedure. Similar experiments have been conducted on Callovo-Oxfordian claystone and its mixtures with bentonite as sealing or backfilling materials (Middelhoff et al. 2020; Zhang et al. 2020). Hence, compacted clays are prepared to ensure the consistency and reproducibility of the experiment.

3.1.2 Compacted clay specimens

Depending on the mineral composition of the rocks from the site, two types of clay materials A and B are used to prepare compacted clay specimens. QXRD is also applied to determine the mineralogy of clay materials. Clay A and Clay B contain similar quartz content but significantly differ in other species, particularly in their clay minerals. **Fig. 2**b indicates that the dominant clay mineral in Clay A is montmorillonite (26.7%), while the clay minerals in Clay B mainly consist of kaolinite (32.1%) and illite (17.8%). These three minerals are representative of the main clay minerals identified in the rock. Clay materials are mixed with sand in pre-determined proportions and thoroughly blended to reproduce a mineral composition comparable to that measured from rocks. **Table 1** lists the mineralogy of the rock discs and the compacted clays, following the preparation work in **Fig. 2**a.

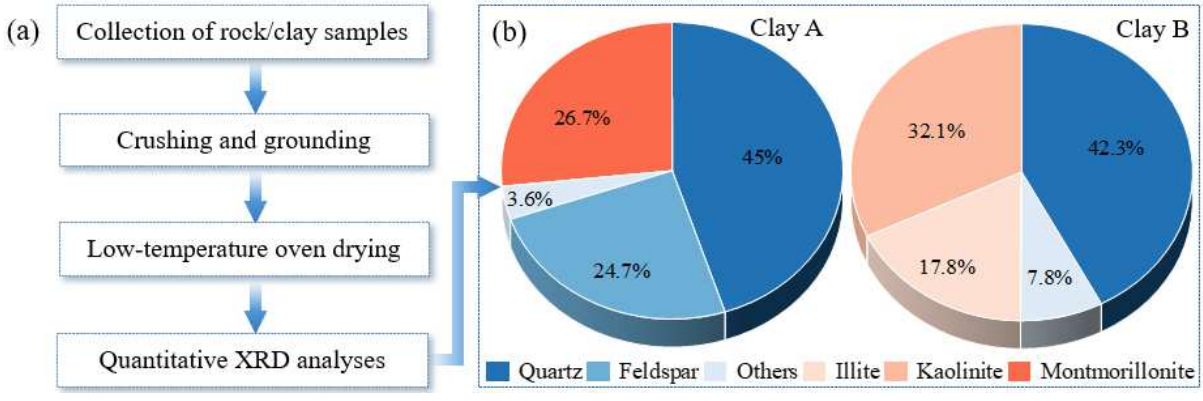


Fig. 2 a Workflow for quantitative XRD analyses **b** Mineral compositions of clay materials A and B

The mixture is prepared within a cylindrical mould with a flexible base and is compacted by a hydraulic press at a controlled rate to achieve the target density. Multiple loading cycles are applied to minimise the rebound of clay minerals during compaction and the potential effects on specimen integrity. The average dimensions of compacted clay are comparable to those of intact rock discs. The dry density of the compacted clay ranges from 1.90 to 1.95 g/cm^3, reaching the maximum density achievable through the described compaction procedure. Compacted clays

are slightly less dense but have a clay content similar to that of the intact rock. The initial water content is assumed to be zero due to the oven-drying process.

Table 1. Mineralogical compositions by weight percentage (wt.%) of rock discs and compacted clays

Minerals	**Rock disc specimen (wt.%)**	**Compacted clay specimen (wt.%)**
Quartz	61.2	61.0
Feldspar	13.1	12.4
Clay minerals	24.0	24.7
Montmorillonite	13.5	14.7
Kaolinite	6.8	6.4
Illite	3.7	3.6
Others	1.7	1.9

2.2 Preparation of salt solutions

Salt solutions are prepared to investigate the effects of water chemistry on clay and rock swelling. The experiments select typical swelling stabilisers, sodium chloride (NaCl), potassium chloride (KCl), and calcium chloride ($CaCl_2$) (Barman and Dash 2022; Murtaza et al. 2025). The swelling properties of specimens are evaluated in the presence of chloride salts. The test in deionised (DI) water serves as a benchmark for the influence of solution chemistry.

The salinity remarkably varies across different rock types under various testing conditions. For example, 0.1 mol/L KCl and NaCl solutions are used to characterise the swelling properties of bentonite (Xiang et al. 2020; Zhang et al. 2024). Higher concentrations, a 1.5 mol/L KCl solution is applied for kimberlite (Morkel and Saydam 2008), and a 5 mol/L NaCl solution is used for Tournemire shale (Wakim et al. 2009) in free swelling tests. This study selects 0.1, 0.5, and 1.0 mol/L, considering the potential detrimental effects of excessive chloride salts in practical applications. For simplicity, the unit mol/L is denoted as M hereafter. Salt solutions of the desired concentrations are prepared by dissolving weighted solid salts in DI water and mixing thoroughly. A dilution process is required to obtain lower-concentration salt solutions. Aqueous mixtures are stored in clean and sealed plastic containers to prevent volatilisation and contamination.

3.3 One-dimensional swelling tests

One-dimensional (free) swelling tests are proposed and broadly employed to measure the lateral-confined swelling behaviour of expansive soils and argillaceous rocks (ASTM 2021; ISRM 1999; Pimentel 2015). This study applies swelling tests under (i) immersion conditions and (ii) wetting and drying cycles. The experimental setup, including apparatus and specimen dimensions, is identical for both testing conditions. For each test, the specimen is placed into a cylinder mould for lateral confinement, with a dial gauge attached at the top for measurement. The test starts as the prepared solution is added to the mould and continues for the designated duration. The axial swelling strain of the specimen is expressed as $\Delta h/h_0$, where h_0 denotes the initial specimen height and Δh denotes the variation in specimen height.

3.3.1 Swelling tests under immersion conditions

The purpose of soaking the specimen is to replicate the constant exposure of geomaterials to a wet environment, such as prolonged contact with groundwater. The dry specimen is fully submerged in DI water or salt solution throughout the test duration. DI water is obtained by removing all ions dissolved in water using a purification system, which ensures purity and consistent ionic conditions, thereby minimising the potential impact of trace ions in distilled water. The axial displacement of specimens is measured using a dial gauge to observe the rate and magnitude of expansion caused by swelling over time. Data are collected to depict the swelling curve and calculate the swelling index (ratio) after the test is terminated.

3.3.2 Swelling tests under wetting and drying cycles

Previous research has noted that cyclic drying and wetting induce volume increases and accelerate deformation, attributed to breakage and disaggregation of the rock structure and the formation of new microcracks during cycles (Pejon and Zuquette 2002; Vergara and Triantafyllidis 2015). Repeated drying and wetting can replicate the cyclic degradation of rock led by watering and de-watering processes in the field (Doostmohammadi et al. 2009; Jiang et al. 2022). Therefore, given the potential influence on the maximum swelling potential of the specimen, wetting and drying cycles are considered following immersion tests.

Fig. 3 demonstrates the experimental procedures of swelling tests with cyclic wetting and drying cycles. The first wetting process, stage A, is conducted by submerging the specimen into DI water and monitored for 20 h. In stage B, the wetted specimen is placed in an oven for 24 h to allow moisture redistribution and evaporation, completing the first cycle. The second wetting process, stage C, is performed by spraying DI water or saturated salt solution on the specimen surface, followed by a 20 h observation period. After treatment, the specimen is oven-dried again for 24 h during Stage D. The final wetting process, stage E, is conducted by immersing the specimen in DI water for 40 h, indicating the completion of cycles. The cycles are intended to replicate moisture fluctuations that trigger swelling. Measurement data are compiled to generate swelling curves versus elapsed time. The measurements of axial strain during oven-drying periods are excluded from the elapsed time presented in the swelling curves.

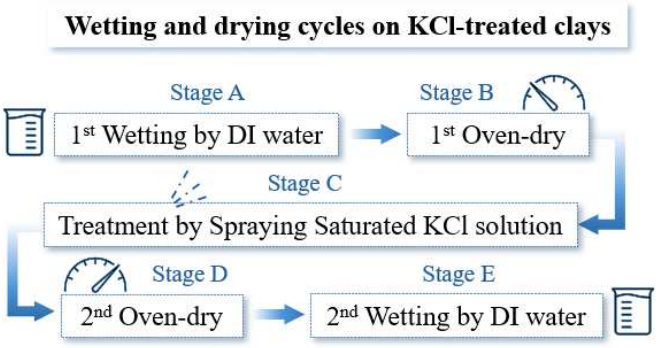


Fig. 3 Experimental procedure for wetting and drying cycles with spraying chemical treatment.

3.4 Microscopic analyses

Microscopic analyses are performed using scanning electron microscopy equipped with energy-dispersive X-ray spectrometry (SEM-EDS). The rock fragment is dehydrated and thinly coated by carbon or gold before scanning

to ensure safe and accurate imaging under vacuum conditions. A Hitachi TM4000Plus benchtop SEM, equipped with a tungsten filament, is employed to capture the surface topography and texture on the rock surface at the nanoscale. The instrument is operated with a backscatter electron (BSE) detector under standard vacuum mode and 15 kV accelerating voltage. High-resolution images are acquired to visualise the morphology and aggregation or clumping of minerals. Magnification for each scan needs to be adjusted according to the resolution required for microstructural details.

Supported by X-ray, EDS enables quantitative elemental analysis and composition mapping on the rock surface. Selected elements are identified and mapped for mineral distribution in the area of interest. Based on XRD results, the distribution of key compositions can be inferred from unique elements. The relative abundance of elements visualises the participation of chemical agents and correlates with macroscopic observations in the laboratory. For SEM-EDS mapping, the operating setting is adjusted to a Bruker Quantax75 detector and 20 kV accelerating voltage. As the contrast and brightness of images are confirmed, the software Bruker Esprit can automatically process data and generate mappings for detailed microscopic investigations.

4. Results and discussion

4.1 Swelling behaviour of compacted clays

4.1.1 Effects of cation type

Swelling tests are first conducted on compacted clays to examine the effects of different cations. **Fig. 4**a reveals the axial strain of the clay specimen in DI water and 1 M solutions of KCl, NaCl, and $CaCl_2$. The presence of K^+, Na^+, and Ca^{2+}exhibit mitigation effects on swelling strain at t = 45 h, compared with DI water. KCl has the most pronounced influence, surpassing the other two at the same concentration, which reduces the strain by 40% (from 59.7% to 35.6%) upon completion of the test. NaCl and $CaCl_2$ have relatively limited impacts, decreasing the swelling strain by 10% and 12%, respectively.

Cation exchange reactions can explain the clay swelling behaviour during soaking in aqueous solutions. Earlier research on ion-exchange reactions revealed that, divalent cations $Ca^{2+}$and Mg^{2+} with two positive charges typically form stronger bonding with negatively charged clay layers compared to monovalent cations $K^+$and Na^+, and thus are expected to produce enhanced swelling inhibition (Barman and Dash 2022; Karami et al. 2023). However, in this study, Ca^{2+} (resulting in 52.2% strain) is less impactful than K^+(resulting in 35.6% strain), indicating that the performance of the swelling inhibitor is not solely governed by cation valence.

One possible explanation is that sodium montmorillonite is the predominant clay mineral in the tested specimen, which has a higher swelling potential. It can be described as Na^+being partially replaced by Ca^{2+}, transforming Na-montmorillonite into Ca-montmorillonite, which exhibits a lower swelling capacity but remains expandable upon exposure to saline environments (Alzamel et al. 2022; Shehata et al. 2021). Reduced swelling control by $CaCl_2$ is validated in experiments on sodium-rich bentonite (Ma et al. 2024; Yunus et al. 2012), supporting this hypothesis. The minor effects of NaCl relative to KCl are attributed to the fact that the hydrated radius of the sodium ion is greater than that of the potassium ion, causing less swelling suppression (Mehdizad et al. 2022). Furthermore, NaCl is less impactful than $CaCl_2$ at the same cationic concentration, as its lower valence and higher

water activity (provides more free water) constrain its ability to resist expansion (Chai et al. 2014). It can be concluded that one-dimensional swelling of the clay is most suppressed by KCl, followed by $CaCl_2$ and NaCl, at 1 M concentration.

Notably, the strain rates of clay specimens vary with cation type and progress through distinct stages, as plotted in **Fig. 4**b. The strain rates are measured at specific time points, i.e., at t = 5, 25, and 45 h. All clay specimens exhibit pronounced deformation rates initially, while as swelling progresses, clay behaviour differs in response to soaking in DI water and soaking in saline solutions. The strain rates of clay specimens submerged in salt solutions sharply decrease from t = 5 h to t = 25 h compared to those treated by DI water, indicating the swelling-stabilising effect of chemical solutions. In subsequent stages, the declines continue but become less noticeable as the test approaches t = 45 h, where most strain rates fall below 0.01 mm/h. Overall, the chemical plays an important role in the early stage and stabilises the clay swelling in a shorter period, whereas the effects of DI water persist for a more extended period and lead to greater deformations at t = 45 h, as shown in **Fig. 4**a.

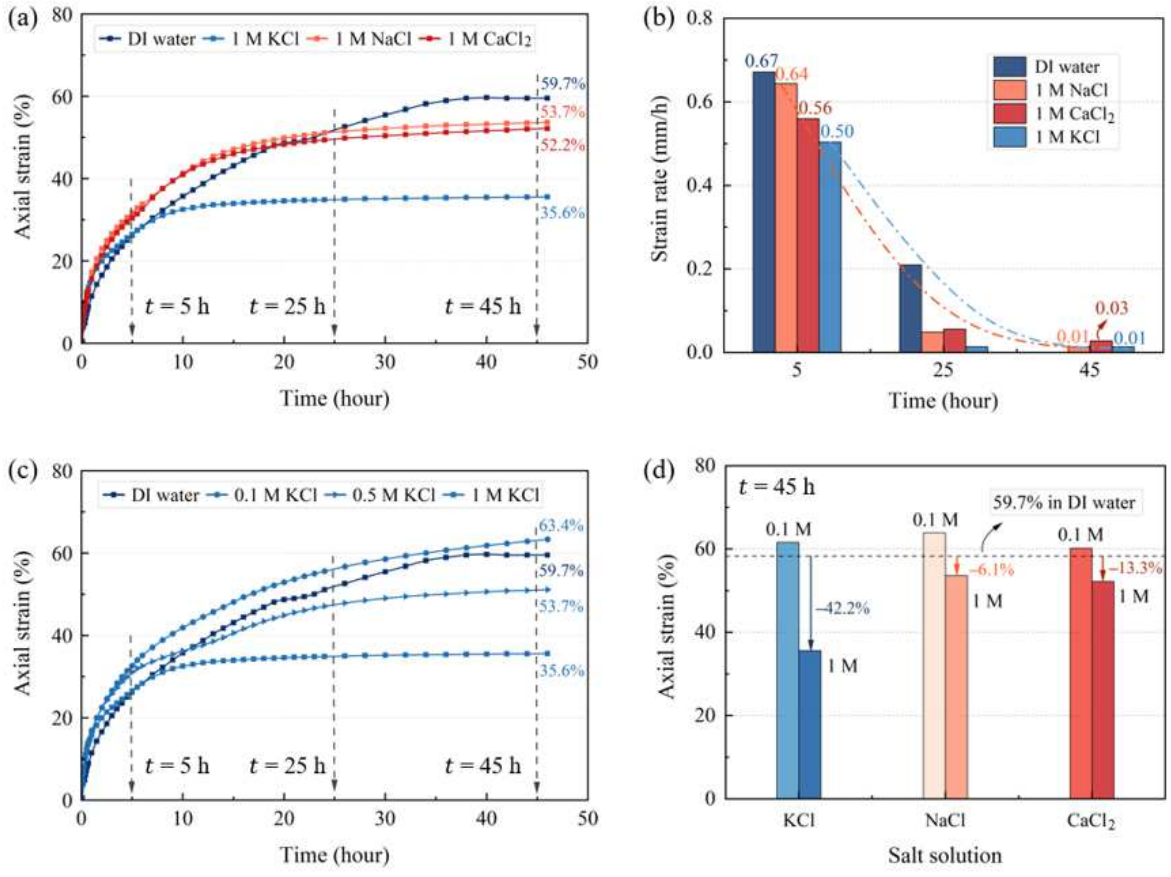


Fig. 4 a,b: clay specimen swelling in DI water and 1 M KCl, NaCl, $CaCl_2$ solutions; **c,d**: clay specimen swelling in DI water and 0.1, 0.5 and 1.0 M KCl solutions.

4.1.2 Effects of cationic concentration

The effects of cationic concentration in immersion tests should also be addressed. Based on previous experiments, $K^+$is more effective at modulating clay swelling relative to $Na^+$and Ca^{2+}. Therefore, KCl is first selected to examine the impacts of cationic concentration on the swelling responses of the clay, followed by NaCl and $CaCl_2$,

as plotted in **Fig. 4**c and d. Increasing the cationic concentration in saline solutions affects both the magnitude and rate of deformation. The variations among KCl solutions at varying concentrations in **Fig. 4**c denote distinct impacts on the axial strain at test termination. Specifically, 0.1 M KCl solution surprisingly accelerates the expansion, resulting in a higher swelling ratio, 63.4%, compared to 59.7% in DI water.

A possible explanation is that, in dilute saline conditions, cations from the bulk solution promote ion exchange and cation mobilisation within the interlayer space between clay particles. This process induces a greater osmotic pressure gradient and establishes a more pronounced Donnan equilibrium, enlarging the spacing between clay platelets and causing more expansion than DI water. This mechanism, known as the Donnan effect, dominates the osmotic swelling of clays (Pusch and Yong 2006). While electrostatic repulsion exists, the osmotic pressure driven by ion concentration difference dominates the driving force separating the clay platelets and controls the overall expansive behaviour of the clay. Accordingly, the most mobile cation Na^+ produces a more substantial Donnan effect, which results in a 63.9% strain in NaCl, higher than the 61.6% in KCl and 60.2% in $CaCl_2$. The comparison between less-concentrated salt solutions and DI water can be found in **Fig. 4**d.

As the concentration increases, water transport is impeded under the combined effect of a reduced osmotic pressure and limited intra-crystalline swelling. Intra-crystalline swelling is hindered as a large amount of cations from high-concentration solutions screens the negative charges on clay surfaces and compresses the electrical double layers, weakening the repulsion force, reducing the interspace between clay platelets, and thus resisting volume increase (Savage 2005). It explains why the axial strain in 0.5 M and 1 M KCl solutions is reduced to 90% and 60% of that measured in DI water.

The effectiveness of concentrated salinity also depends on the type of cations. **Fig. 4**d reveals that a 1 M KCl solution provides enhanced mitigation effects compared to NaCl and $CaCl_2$ at the same concentration. More specifically, as concentration rises from 0.1 M to 1 M, the axial strain is decreased by 42.2% for KCl, 16.1% for NaCl, and 13.3% for $CaCl_2$. Section 3.1.1 discusses why dilute KCl outperforms the other two chloride salts, and the same reasons hold here. However, the results of concentrated NaCl and $CaCl_2$ are opposite to observations in dilute solutions, where a higher concentration of Na^+ is more impactful. As the compression of the electrical double layer is strengthened under concentrated conditions, Na^+, with a smaller hydrated radius, exerts a stronger resistance to expansion. The research applying salt solutions to Na-bentonite (Xiang et al. 2020) also supports this finding. In summary, the outcomes imply that clay behaviour is governed by the combined effects of cation type and its concentration in the aqueous phase.

4.1.3 Effects of wetting and drying cycles

The effects of cyclic wetting and drying are evaluated via swelling tests on compacted clay specimens. The test with DI water serves as a control group for three KCl-treated tests named KCl-1, KCl-2, and KCl-3. For tests with KCl treatment, the first two are conducted in a controlled-humidity system, while the last is subjected to better ventilation conditions. **Fig. 3** describes the cyclic wetting and drying on compacted clay specimens, and the only difference in the control group is that spraying is carried out by DI water. Applying aqueous chemicals is quantified to enable consistency among the tests, with 50 ml of DI water added in the first and second wetting processes and 10 ml of DI water or saturated KCl solution sprayed on the specimen surface during the treatment. The experimental steps are labelled Stage A to E, and the corresponding axial swelling strains of clay specimens are

plotted in **Fig. 5**. The primary focus of **Fig. 5** is to capture the specimen's expansion behaviour. Therefore, the time spent on oven-drying within each cycle is excluded, which explains the sudden drops in strain curves.

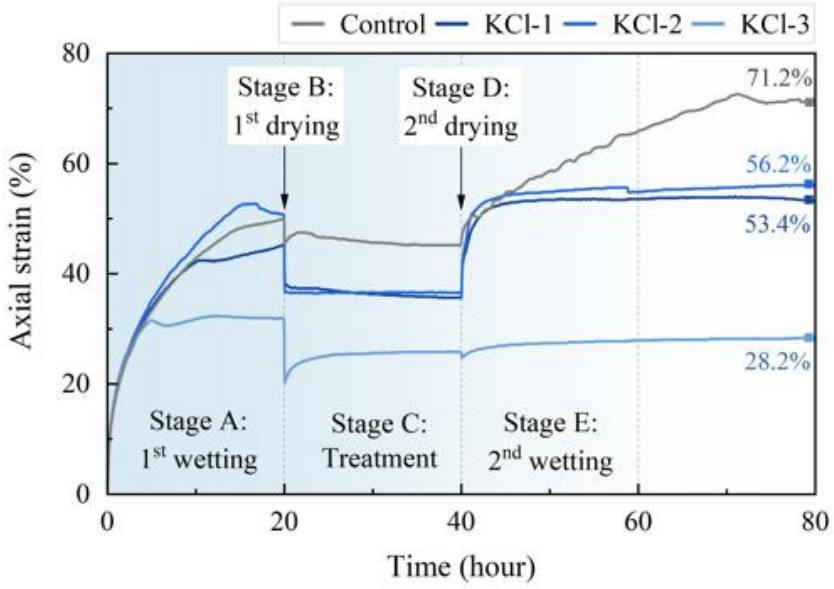


Fig. 5 Swelling strain of clay specimen in the control group and the KCl-treated tests during cycles.

In the control group, the clay vertically expands to half of its initial height by the end of Stage A and shrinks by 5% after drying in Stage B. Stages C and D have minimal effects, while Stage E intensifies deformation behaviour and exhibits an increasing tendency. A more evident swelling response occurs in Stage A for the KCl-1 test, but it becomes negligible after the first drying process. There is a more pronounced difference in the swelling response of post-treatment clay specimens. After spraying chemicals, the strain curves of the KCl-1 test and KCl-2 test settle within a short period in Stage E, which leads to less deformation at the end of cycles, i.e., t = 80 hours. As a result, the swelling strains are decreased by nearly 25% relative to the control group, 71.2%, producing comparable results under identical testing conditions. Remarkably, improved ventilation condition results in lower axial strain in the KCl-3 test. From the early stage of the cycles, around t = 5 h, the KCl-3 test shows a diminished swelling under the persistent effects of local humidity fluctuations. The microstructural changes are illustrated and discussed with reference to **Fig. 6**.

To intuitively investigate clay swelling during cycles, **Fig. 6** characterises the surface features, such as micro-pore formation and crack propagation, providing evidence of microstructural changes. Wetting and drying cycles have been demonstrated to produce an adverse impact on the water retention capacity of clayey soils due to the rapid water inflow and outflow through desiccation cracks and micro-pores (Gao et al. 2023). Observations from **Fig. 6** indicate that the presence of KCl and the ventilation conditions appear to facilitate this process and further reduce the water retention of the clay specimen.

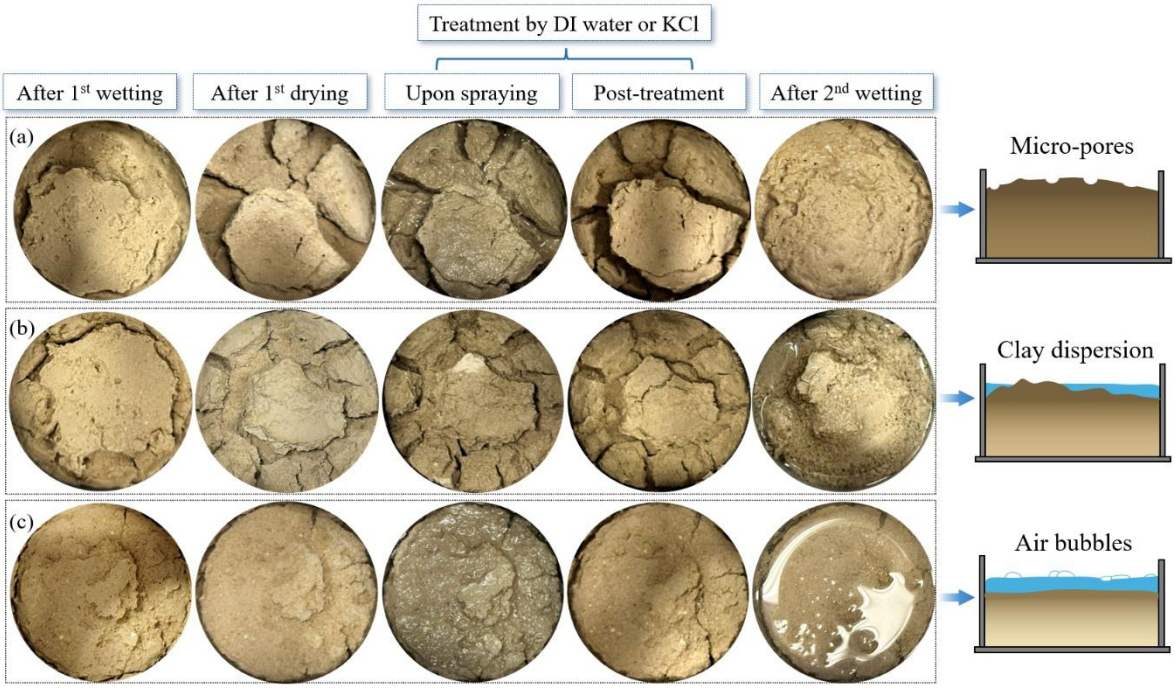


Fig. 6 Surface of clay specimens during wetting and drying cycles in **a** Control group (DI water), **b** KCl-2, and **c** KCl-3.

In **Fig. 6**a, the control group using DI water for treatment performs the most pronounced water absorption ability at the end of cycles. All added water is absorbed by the clay specimen and results in the formation of micro-pores on its muddy and hydrated surface after water uptake, as displayed by the figure after the second wetting process. In contrast, a portion of water remains on KCl-treated specimens upon the completion of the test, suggesting a reduced or impeded interaction between the post-treatment clay specimen and water during the re-saturation process. **Fig. 6**b denotes the breakdown and dispersion of clay aggregates in the KCl-2 test, indicating ongoing interplay between residual water and clay particles. **Fig. 6**c reveals that more water is retained on the specimen surface and forms a visible water layer, where the floating bubbles signify that ongoing infiltration of water into the clay specimen in the KCl-3 test. The bubbles originate from the release or escape of entrapped air when water attempts to infiltrate the permeable surface of the clay specimen.

The pattern and propagation of microcracks vary in different situations. From the first moisturising process to the treatment, radial cracks clearly evidence the expansion and shrinkage of desiccated clay specimens for the control group and the KCl-2 test. Those fractures originate from the boundary and propagate deeper to the central position under the humidity-controlled conditions. Clay forms discrete and irregular clods that are radially distributed after desiccation. Under enhanced ventilation, the KCl-3 test has reduced crack opening and retains more water at test completion. The surface remains intact with fewer radial cracks, while circumferential cracks are still open around the boundary. Moreover, the development and distribution of cracks in the KCl-3 test differ from those in the KCl-2 test from the first wetting, which implies that the influence of the humidity, independent of chemical treatment, modulates clay behaviour from the start of the test. This effect continues because improved ventilation accelerates the water evaporation from the clay surface, thereby retarding crack opening and propagation. This interpretation is also supported by field surveys in clayey formations (Li and Liu 2013; Mayor et al. 2007), ventilation induces

desaturation in the rock near the excavation and promotes evaporation at the excavated surface, thereby reducing humidity and restraining swelling locally.

The quantitative analysis of surface cracks in **Fig. 7** complements the qualitative observations shown in **Fig. 6**. Surface crack parameters are determined to compare the extent and pattern of surface cracking between the control group and KCl-treated groups. These parameters are not used as inputs for subsequent numerical modelling but provide quantitative evidence for assessing the effects of KCl treatment during wet-dry cycles.

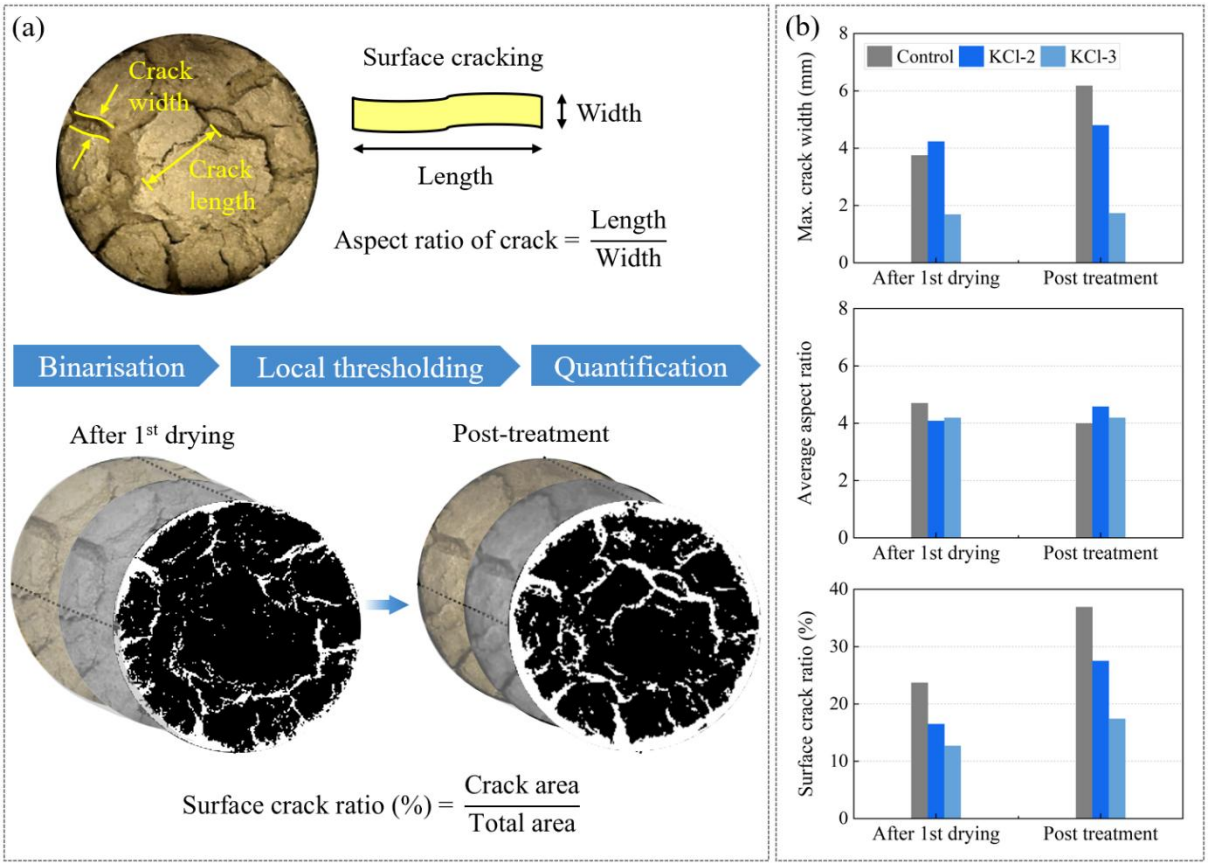


Fig. 7 a Image processing on clay specimens after the first drying and after the treatment, **b** Quantitative analyses of surface cracking

Digital image processing is applied to quantify and evaluate the surface cracking on desiccated clays, as depicted in **Fig. 7**a. Colour images are processed by binarisation and local thresholding for quantifying crack patterns and distribution. The maximum crack width is measured from the widest crack developed after desiccation. The aspect ratio is determined by the ratio of crack length to its width. Surface crack ratio, or crack intensity factor, refers to the proportion of crack area in the total original area of the clay surface (Tang et al. 2011).

From the first wetting to the treatment, spraying water in the control group has a greater impact on existing cracks. The maximum crack width and surface crack ratio increase as existing cracks are widened and deepened. Under controlled-humidity conditions, the extent of surface cracking in the KCl-2 test is diminished relative to the control group. In **Fig. 7**b, the maximum crack width expands by 0.57 mm after spraying KCl, while the untreated crack widens by 2.43 mm. The crack area is enlarged from 16.5% to 27.5% after spraying KCl, while the untreated clay shows expansion from 23.7% to 36.9%. Moreover, the KCl-3 test results suggest that enhanced ventilation further

impedes the formation and propagation of surface cracking, where fewer cracks and less deformation are observed. It should be noted that ventilation and chemical treatment have little effect on the average aspect ratio of cracks. The crack pattern or shape tends to expand or contract proportionally during desiccation. However, as moisture redistributes within the clay, the homogeneity decreases, and the resulting non-uniform distribution of moisture leads to cumulative deformation and loss of structural integrity in the following wetting path.

Fig. 8 provides supplementary data on the accumulation of strains and the variation in strain rate during the final wetting, Stage E. The initial strain is assumed to be zero, as this figure emphasises the expansive behaviour of the post-treatment clay specimen. The effects of swelling stabilisers are assessed based on swelling deformation (left y-axis) and change in strain rate (right y-axis) over time. The control group in **Fig. 8**a, with a continuous expansive tendency, presents the highest swelling potential among all tests on clay specimens. A steep collapse occurring after t = 70 h can be explained by a process analogous to the slaking and disintegration of the claystone upon exposure to water (Nunt-Jaruwong 2006). **Fig. 8**b and c demonstrate that two KCl-treated clay specimens under controlled humidity have elevated strain rates at the onset of Stage E, where the maximum reaches 8.75% per hour, equivalent to a 2.3 mm/h deformation rate. Nevertheless, the strain rate experiences the most remarkable declines in these two cases, leading to the flatter curves after t = 45 h. For the KCl-3 test shown in **Fig. 8**d, under the concurrent effect of ventilation and KCl treatment, the accumulated axial strain at the end of Stage E is substantially diminished, less than one-fifth of the measurement in the KCl-2 test. The finding also validates the contribution of enhanced ventilation to swelling suppression.

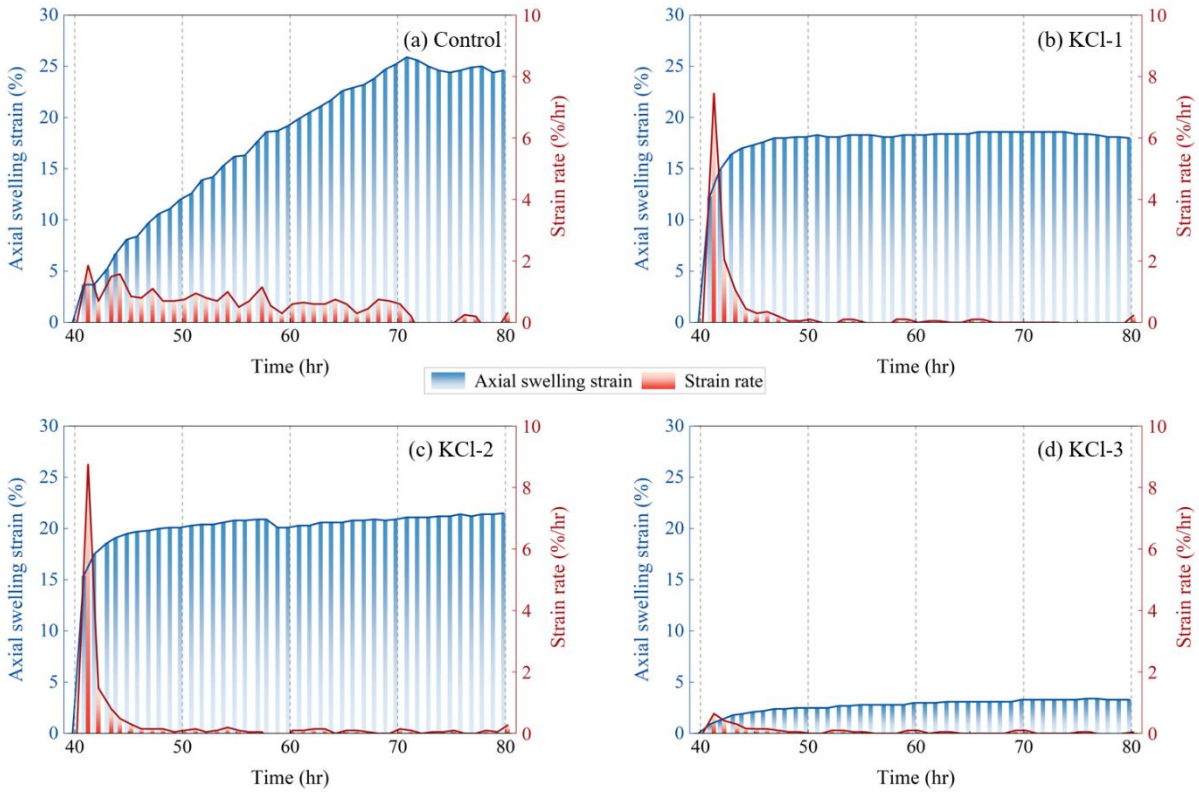


Fig. 8 Axial swelling strains and strain rate of clays during stage E: **a** in control group, **b, c,** and **d** in tests with KCl treatment

In short, spraying a saturated KCl solution on the clay surface can reduce the surface cracking during desiccation. The water retention capacity of the treated clay is decreased, and thus, expansive behaviour stabilises in a shorter period. All KCl-treated clays exhibit reduced swelling compared to the control group, and the effectiveness of spraying KCl can be further improved by altering ventilation conditions. Observations during cyclic wetting and drying on clays inform the treatment design to control rock swelling and highlight the need for more in-depth analyses.

4.2 Swelling behaviour of rocks

Applying chemical solutions to the rock is complicated and challenging to control due to inherent heterogeneity, cementation, and natural fractures of clay formations. In this section, swelling behaviours of rock discs under KCl effects are explored in light of previous experiments on compacted clays.

Experimental work starts from immersion tests conducted on the rock. Rock discs soak in DI water and in different concentrations of KCl solutions. **Fig. 9**a depicts the strain-time relation of the rock specimen in response to 0.1 to 1 M KCl solutions. The maximum axial strain of the rock specimen in the control group only reaches 1.9%, significantly lower than the 71.2% measured in the clay specimen. The clay specimens prepared in the laboratory, even with the same mineral composition, present at least an order of magnitude greater swelling than the rock collected from the site. The finding highlights the differences between intact rock and compacted clay specimens and signifies the underlying mechanisms. One explanation arises from the strengthened rock matrix of tuffaceous claystone collected from the study area, Newcastle Coalfield. Tuff formations originate from volcanic ash deposits and gain strength from consolidation, cementation, recrystallisation, and other diagenesis processes, consisting of essential stratigraphic units in the Newcastle Coal Measures (McNally and Branagan 2014). The stronger bonding and adhesion between grains within the rock formation strengthen the mechanical properties and restrain its ability to expand in water. It reveals why the compacted clay is more vulnerable to swelling, as the compaction process in the laboratory cannot reproduce the in-situ condition that forms strong bonds between minerals.

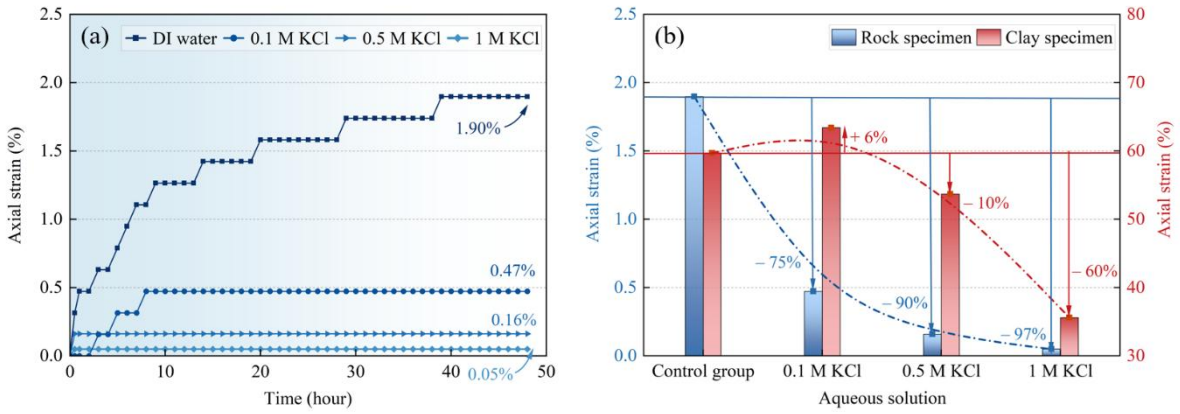


Fig. 9 a Rock swelling in DI water and 0.1, 0.5, 1 M KCl solutions, **b** Comparison of rock and clay behaviour under KCl effects

Another noticeable finding is that the swelling strain of the rock specimen is nonlinearly and inversely related to the solution concentration. **Fig. 9**b points out the reduced efficacy of chemicals in modulating rock swelling. More specifically, 50 ml of 0.1 M KCl decreases the strain by 75%, while the same amount of 0.5M and 1.0M KCl

solutions only provides an additional 15% and 22% reduction, respectively. A non-linear relationship is observed between cationic concentration and control effect. Consequently, the expenditure can escalate since a large amount of salt is required to reach the target concentration, potentially reducing the overall cost-effectiveness.

The influence of diluted salt solutions on rock behaviour is opposite to the observations on clay specimens. In immersion tests, the salt solution intensifies clay swelling at lower concentrations but starts to impede swelling as the concentration exceeds a threshold value, establishing a non-monotonic relationship between axial strain and cationic concentration. Such an association could not be found in experiments on rock specimens. The swelling of rock specimens shows a continuous non-linear decline once the salt solution is introduced into the test. This contradiction signifies the differences between the rock and clay specimens in a low-salinity environment, which is governed by the competition between osmotic swelling and intra-crystalline swelling (Madsen and Müller-Vonmoos 1989). For intact rock specimens, the latter dominates the interaction of water and clay minerals and is less influenced by the chemical agent. The strong cohesion or cementation between the minerals within the rock matrix restrains the osmotic swelling described in Sect. 3.1.2, constraining water movement/inflow. Accordingly, KCl only provides mitigation effects on rock specimens, even though it plays an important role in osmotic swelling.

4.3 Microscopic observations on rock swelling

4.3.1 SEM scanning

Microstructural changes on the specimen surface are difficult to observe directly due to the limited volumetric expansion of the rock. Detailed characterisation is required to capture the invisible changes of the specimen before and after the treatment, complementing the macroscopic observations in swelling tests. The micro-level analyses also support the solid interpretation of underlying swelling mechanisms under chemical effects. Therefore, the microscopic technique is typically chosen for the detailed analyses at a finer scale, in micrometres, to observe the swelling evolution in water or salt solutions (Murtaza et al. 2025; Zhang et al. 2024).

In this section, rock fragments are selected for high-resolution imaging and semi-quantitative elemental analyses using SEM and SEM-EDS. The specimens were not polished prior to scanning to preserve the morphological features induced by swelling. Microscopic analyses are conducted on rock fragments: (i) before swelling, (ii) after immersion in 1 M KCl solution, and (iii) after immersion in DI water. The corresponding tests are labelled dry, KCl and DI water. Micro-level imaging attempts to capture the surface morphology and microstructural features of the rock before and after the interaction with water or chemical additives. The potential influence of KCl is discussed to interpret the observed macroscopic swelling. **Fig. 10** illustrates the workflow of the microscopic investigations and subsequent analyses.

SEM scanning on rock materials characterises the structural and textural features by greyscale images. The images are processed by Python programming to extract two-dimensional intensity profiles along X-Z and Y-Z directions, where X and Y denote the longitudinal (1000 pixels) and transverse (800 pixels) directions. Z value refers to the pixel/greyscale intensity falling from 0 in black to 255 in white, where the grey value (height in z-direction) is expressed as a function of pixel locations in the images (Gao et al. 2023). Multiple intensity profiles are assembled to generate three-dimensional intensity plots for the overall intensity variation across the scanned area.

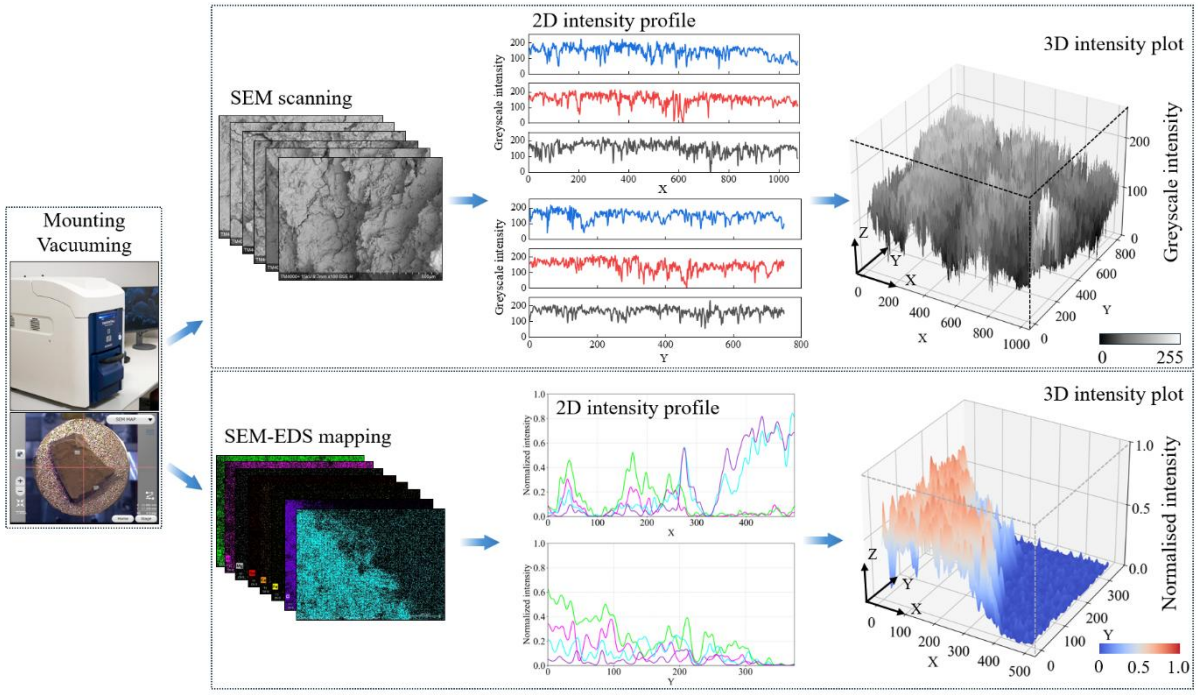


Fig. 10 Microscopic investigations and associated analyses on rocks, supported by SEM and SEM-EDS

The selection of the scanning area and settings affects the resolution and accuracy of greyscale images, particularly for coarse specimen surface. **Fig. 11**a displays the images under 100× magnification for a broader view of the microstructural features across the scanning area. The dry rock exhibits an intact structure with visible boundaries, whereas the water-submerged one shows apparent micro-cracks and fragmented particles at the boundary regions. The observations reveal that the disintegration or rearrangement of mineral aggregates significantly increases the surface roughness. The roughened surface exposes more mineral clumps to water, thereby exacerbating swelling, which aligns with the most pronounced swelling responses observed in DI water. Notably, a "layered" or "coating-like" surface covers the KCl-treated rock, resulting in more textural contrasts and clearly defined boundaries. **Fig. 11**c depicts 3D intensity plots derived from images in **Fig. 11**a complements the experimental observations by quantifying greyscale variations.

In the same area, finer microstructure details are characterised by 1000× scanning magnification, as displayed in **Fig. 11**b. The distribution of "flaky" aggregations is more evident for dry and KCl-treated rocks at enhanced resolutions. However, the layered structure appears less distinct and difficult to distinguish rocks before and after swelling. **Fig. 11**d illustrates intensity plots derived from images in **Fig. 11**b, where the contrast is reduced relative to low-concentration scans. It is essential to quantify the scan results while accounting for the potential effects of imaging magnification. In addition, some high-contrast particles are detected on the rocks after soaking in water and KCl. The detected bright particles are precipitates or crystals when minerals react with water and remain on the rock surface after drying. The composition and property of bright particles need to be determined by elemental analyses supported by SEM-EDS.

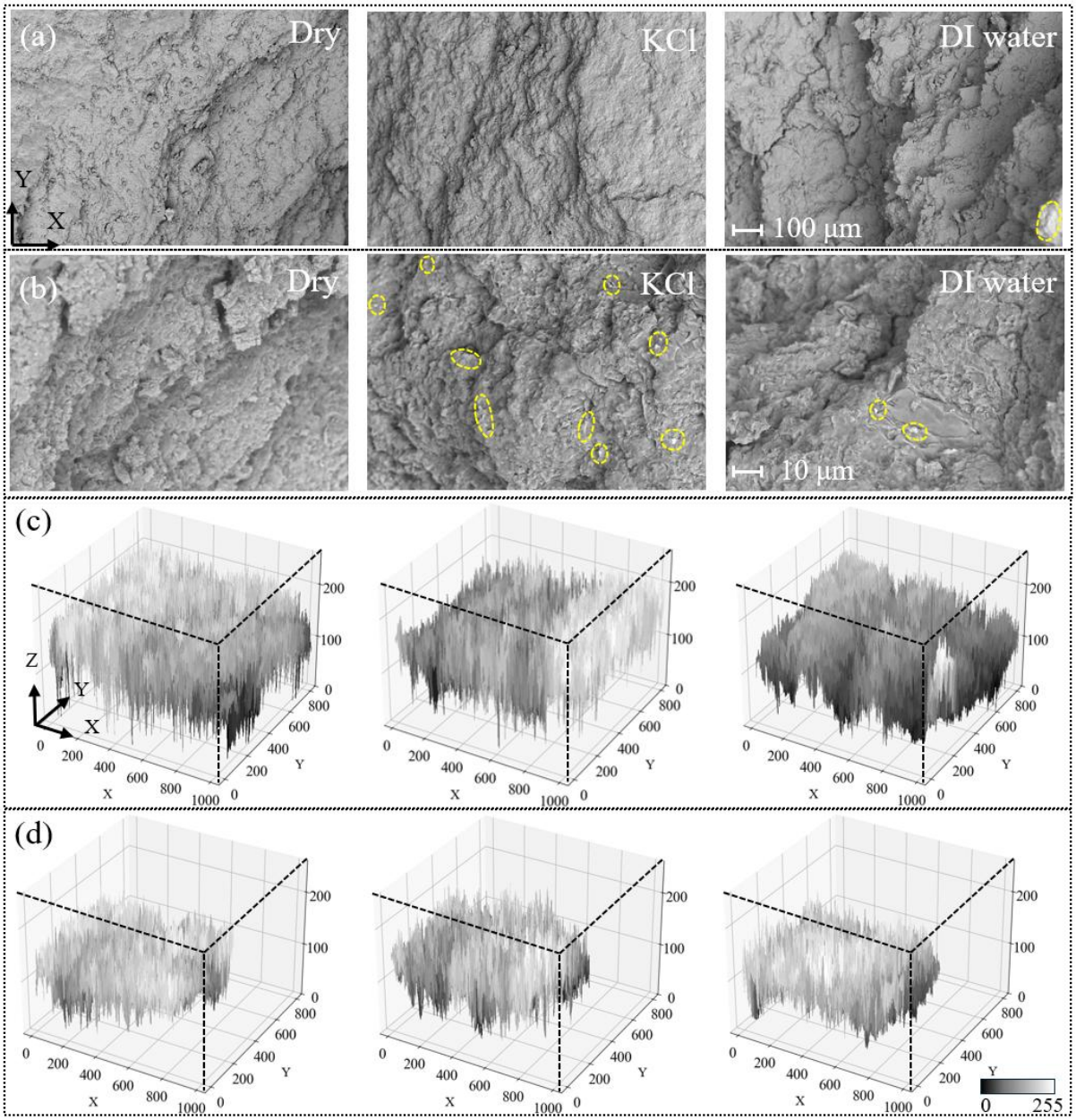


Fig. 11 SEM scans of rocks at **a** 100× and **b** 1000× magnification, with corresponding 3D intensity plots shown in **c** and **d**. Grayscale intensity ranges 0 to 255 and is dimensionless.

To quantify surface roughness, the intensity plots are processed to determine the areal roughness parameters of SEM images. The parameter S_a defines the arithmetic mean height, and S_q defines the root mean square height of surface roughness over the measured area (He et al. 2021; Rosentritt et al. 2024), as expressed in Eq.1 and Eq. 2.

$$S_a = \frac{1}{MN}\sum_{i=1}^{M}\sum_{j=1}^{N} z(x_i, y_i) \tag{1}$$

$$S_q = \sqrt{\frac{1}{MN}\sum_{i=1}^{M}\sum_{j=1}^{N} z(x_i, y_i)^2} \tag{2}$$

where M, N refer to the number of pixels in X, Y directions, and $z(x_i, y_i)$ refers to the height deviation from the reference plane in Z-direction. The calculation is repeated for images from dry, KCl, and DI water tests. At least five images are processed at each magnification, i.e., 100×, 300×, 1000×, and 2000×. **Fig. 12** summarises the mean values of S_a and S_q on the left y-axis, while their variations, expressed as ΔS_a and ΔS_q, are plotted on the right y-axis. Scans from KCl (in blue) and DI water (in red) tests have higher average intensity values of S_a and S_q than those on dry rocks, indicating greater surface roughness of the rocks after swelling. Moreover, the intensity values calculated from the KCl tests are comparable to those in DI water tests. It implies that wetting-induced alteration dominates the variations in surface morphology, while the contributions of different aqueous phases are difficult to discern solely based on roughness parameters.

The relationship between roughness parameters and imaging magnification should be addressed. Although higher scanning scales reveal finer microstructural details, the variation in surface morphology caused by swelling is not significantly enhanced by increasing magnification. For example, in **Fig. 12**a, the difference between dry and KCl tests ΔS_q decreases from 9.9 at 300× magnification to 5.3 at 2000× magnification. A slower reduction is present between dry and DI water tests, more specifically, ΔS_q declines from 8.2 to 7.3. Non-linear relationships are also observed in **Fig. 12**b, suggesting that the contrast in surface roughness does not improve as imaging magnification increases. The findings from SEM images convey valuable insights into the morphological features of the rock surface and necessitate further investigations to assess rock behaviour in DI water versus salt solutions.

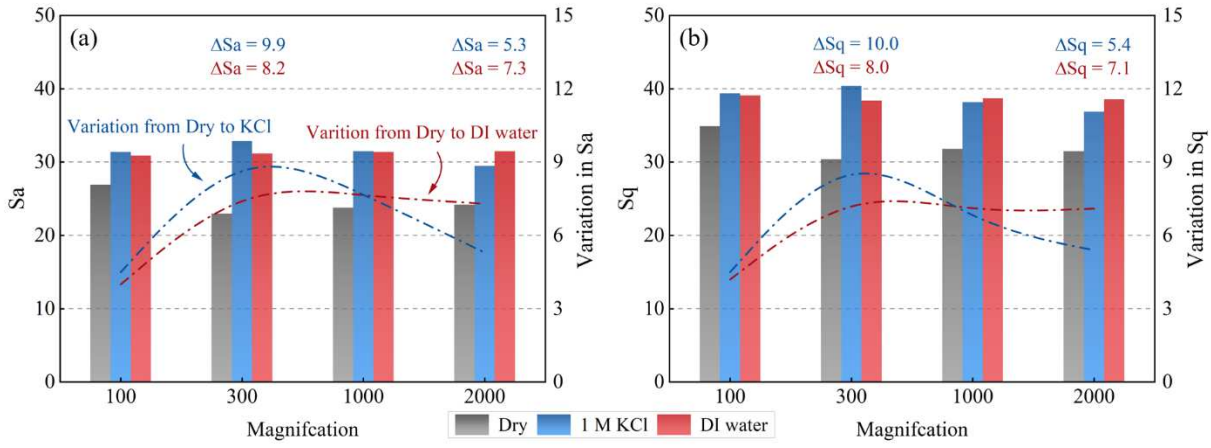


Fig. 12 a Arithmetic mean and its variation S_a, ΔS_a, **b** Root mean square and its variation S_q, ΔS_q, determined from SEM images

4.3.2 SEM-EDS mapping

Following the evaluation of surface topography, EDS enables the semi-quantitative identification of elemental compositions within the region of interest. The integration facilitates interpreting macroscopic observations from swelling tests and identifying high-contrast regions in SEM images. The collaboration serves to examine the function of water or salt solution in clay mineral swelling through multiscale analyses. After pre-conditioning, involving oven-drying and coating, the rocks are scanned with an X-ray detector activated under high vacuum conditions. EDS mappings are operated under 100× magnification. **Fig. 13** shows the distribution and abundance of Si, Al, K, and Cl by single-element maps of rocks after 24-hour immersion in DI water and 1 M KCl solution. Key elements are selected based on the mineralogical composition results from XRD.

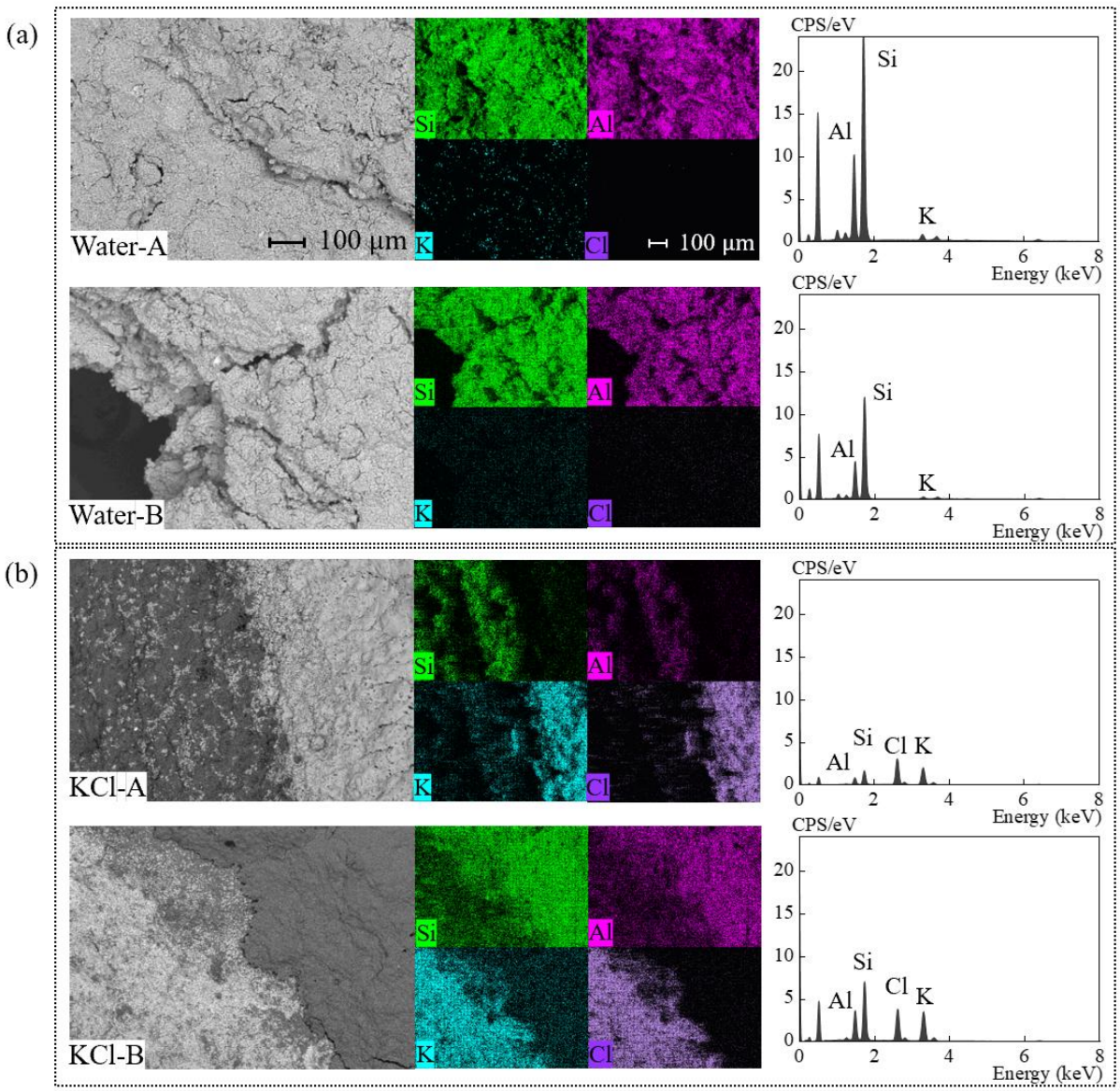


Fig. 13 Spectrum and element maps of rocks after 24-hour immersion in **A** DI water and **B** 1 M KCl solution

Mappings on rocks after immersion in DI water are labelled as Water-A and Water-B. **Fig. 13**a selects the scans from a relatively intact region (upper) and the edge of the rock surface (lower). The spatial patterns of Si and Al are strongly overlapping and delineate the distribution of the main aluminosilicate minerals (quartz, feldspar), whereas K and Cl are less informative for mineral identification and have negligible contributions to the overall composition. Micro-cracks are well propagated near the boundary, and no apparent high-contrast regions are found. **Fig. 13**b shows spectrum and EDS mapping on rocks after immersion in 1 M KCl solution. The region of interest is chosen from areas with enhanced contrast, similar to high-contrast particles noted in greyscale scans. Notably, K and Cl extensively coincide with brighter areas in SEM scans, and the strong correlation of K and Cl is validated by the X-ray spectrum. Furthermore, K and Cl are distinct from or less concentrated in the dense regions of Si and Al. The segregation phenomena reveal substantial variations in elemental abundance across the scanning area, revealing that precipitation or crystallisation may form and be non-uniformly distributed within the bright areas.

Accordingly, the elemental abundance or intensity needs to be quantified to evaluate the potential correlations among key elements within the scanning area.

Fig. 14 presents the normalised elemental intensities acquired from the middle positions in horizontal and vertical directions, based on KCl-A and KCl-B scans in **Fig. 12**. The line profiles are illustrated in the same colour as the single-element maps. The evidence indicates the correlations between different compositions within low-contrast and high-contrast regions. Higher intensities of K and Cl are observed in adjacent areas, such as at x ranging from 350 to 500 pixels in **Fig. 14**a, corresponding to the brighter regions in greyscale scans. In addition, a decreasing trend in K and Cl is observed close to the distinct boundary at the central position at x equals 250 pixels in **Fig. 14**b. The elemental characterisation for individual profiles is representative of key compositional variations and indicate the possible compounds in the bright regions observed in SEM images.

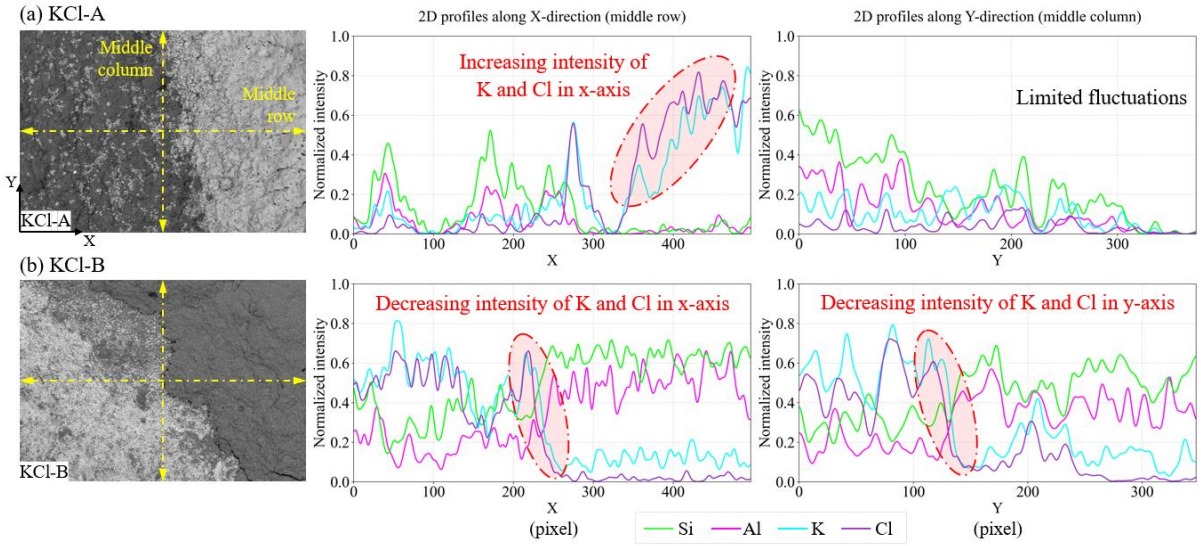


Fig. 14 Two-dimensional profiles of normalised elemental intensity at the middle of **a** KCl-A and **b** KCl-B scans

Fig. 15 reconstructs the normalised intensities of the selected elements into three-dimensional plots by stacking multiple individual profiles. Elemental distributions are quantified using a colour contrast ranging from blue to red along the z-axis. Similar to **Fig. 14**a, K and Cl are densely distributed from x equals 350 to 500 pixels in **Fig. 15**a, with an average normalised intensity exceeding 0.5. In **Fig. 15**b, K and Cl are found in close association and are clustered in the brighter area of the SEM images, clearly contrasting with the darker regions. In comparison, Si and Al coexist in certain regions, but the coexistence is less pronounced and difficult to evaluate due to the widespread occurrence of aluminosilicate phases. The mapping of Si and Al can supplement information on the compositional variations, particularly in areas with lower K and Cl concentrations.

Three-dimensional intensity plots provide enhanced visualisations and interpretations of the spatial correlations of the selected elements. The co-occurrence of those elements suggests that some precipitations form and deposit from saline environments. However, the occurrence of salt crystals or precipitations warrants additional attention. There are two possible explanations for the KCl crystal formation. Firstly, a surface coating or barrier forms as the residual or “unreacted” salts settle and shield the rock surface after swelling, which explains the coating-like crystalline observed in **Fig. 13**b. The barrier prevents excessive water uptake by clay minerals, weakening the expansion behaviour triggered by the re-saturation process. Such phenomena may not occur or be less frequent

under practical conditions due to the high solubility of salt solids. This interpretation may not directly prove the mitigation effects of chemical additives but still identifies the KCl participation. Another explanation is that the salts precipitate during the water evaporation process, as oven-drying is required before scanning. The non-uniform distribution of salt crystals suggests the solution migration across the surface during the drying process, which also reflects the movement of K^+ in cation exchange reactions and osmotic swelling. The dispersive KCl crystals could be attributed to the heterogeneous distribution of swelling minerals.

Overall, micro-scale analyses using SEM and EDS deliver valuable perspectives on rock swelling under chemical effects and highlight the importance of future studies with less sample preparation disturbance. Micro-CT, with non-destructive sample preparation, enables 3D visualisation of internal structure and monitors its changes during rock swelling. Time-dependent swelling is better captured through spatial scanning and associated data processing, including registration and segmentation. Changes in pore sizes, shape, and connectivity facilitate the evaluation of porosity and permeability variations as swelling occurs in different aqueous environments. The integration of micro-CT and EDS allows for improved spatial characterisation of swelling behaviour within rocks and, therefore, is recommended for future studies.

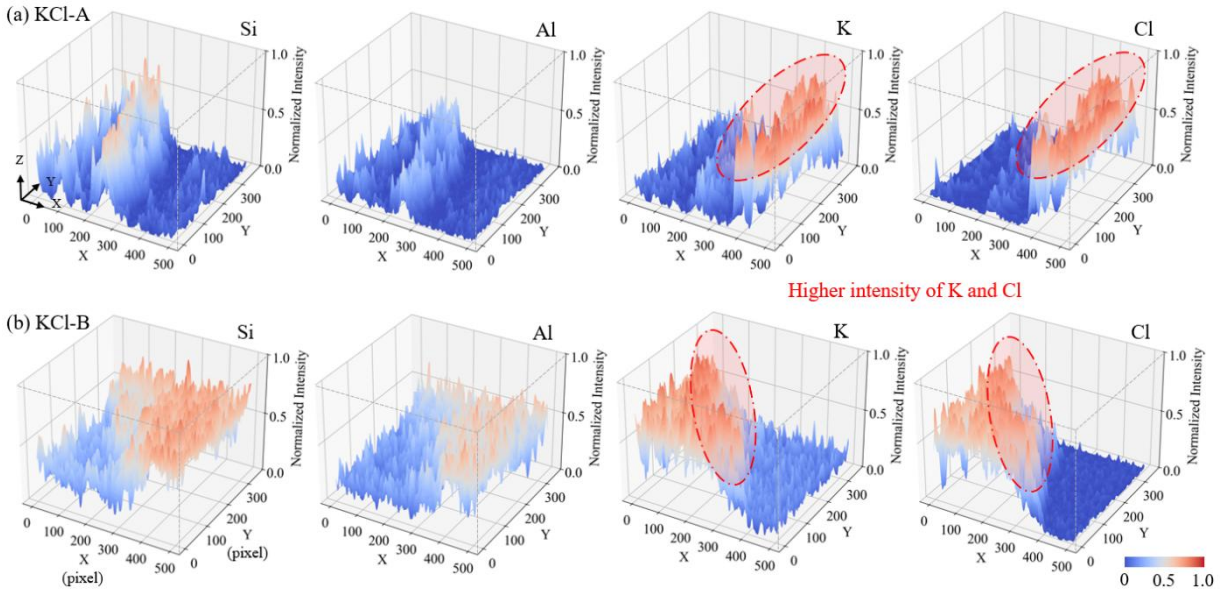


Fig. 15 Three-dimensional plots of normalised elemental intensity in **a** KCl-A and **b** KCl-B scans

5. Practical considerations

5.1 Assessment of rock durability

The experimental results and analyses emphasise the chemical effects on rock behaviour in conditions conducive to degradation and breakdown. In field conditions, rocks can disintegrate and collapse upon long-term exposure to air and moisture, threatening the structural integrity and operational safety. The geo-durability classification proposed by Olivier (1979) aims to distinguish durable and non-durable using two index parameters, the uniaxial compressive strength and free swelling coefficient, the latter of which is measured by the test proposed by Duncan et al. (1968). The classification provides a rating system that ranges from class A with excellent durability to class F with very poor durability, which is designed to assess the rock's resilience to weathering and slaking in the field.

The classification provides an additional criterion to evaluate the impacts of chemical treatment. **Fig. 16** compares the ratings of the rock before and after KCl treatment, with samples taken from the same drill core. The average uniaxial compressive strength is determined as 55 MPa. Rocks in DI water are mainly located in durability rating from moderate poor to very poor, whereas rocks after KCl treatment are more clustered within the class of good to fair. KCl exerts positive impacts and improves the durability of the rock against weathering and deterioration. The competence of KCl treatment on rock does not follow a linear relationship with solution concentration, which is attributed to the heterogeneous distribution of swelling minerals within the rock, and changes in porosity and permeability as swelling progresses. Nevertheless, the KCl treatment produces a consistent impact that improves rock durability. The geo-durability classification validates the contribution of chemical treatment and offers new insights for rapid assessment of nondurable rocks in swelling-prone field conditions.

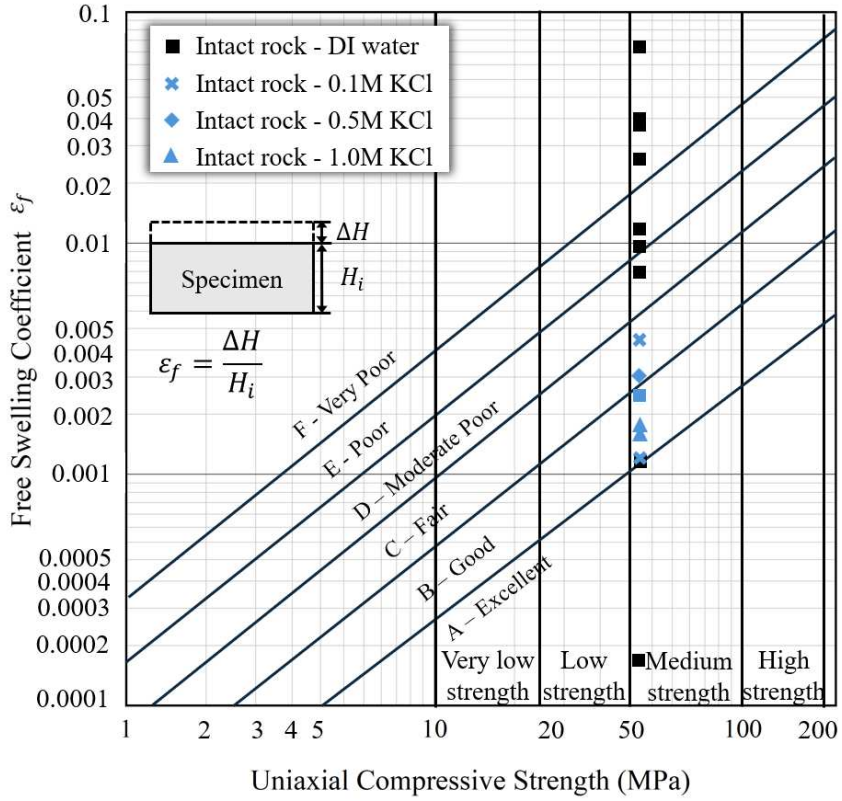


Fig. 16 Application of geo-durability classification on rocks before and after KCl treatment, after Olivier (1979)

5.2 Potential impacts of groundwater chemistry

Based on swelling test results, the cation concentration plays a vital role in the extent and rate of clay swelling. Under field conditions, the groundwater compositions are substantially more complicated than those prepared in the laboratory. Chemical analysis of groundwater samples would help identify the field conditions susceptible to swelling and contribute to effective strategies for swelling prediction. Hence, groundwater samples collected from the floor heave area at the site are delivered to the analytical centre for Inductively Coupled Plasma - Optical emission Spectrometry (ICP-OES) analyses. ICP-OES aims to determine the composition and concentrations of dissolved species in the tested water sample. The method detection limit ensures 99% certainty, enabling reliable identification and quantification for geochemical characterisations of groundwater from the study area.

Fig. 17 compiles the major elements identified in groundwater samples from this study, Shultz (1988), and Whittall (1990). Groundwater samples were collected from the goaf outflow in areas affected by excavations. The most widespread distribution lies in the composition of dissolved Na^+, where the maximum ion concentration approaches 800 mg/L, equivalent to 0.035 mol/L. The greater Na^+ concentration typically indicates a saline environment that promotes swelling, allowing more Na ions to enter the inter-layer spaces of montmorillonite and trigger expansion. Other cations are more clustered at lower concentrations, less than 100 mg/L. Element Ca and Mg are generally recognised as key indicators of carbonate minerals. Element K, Fe, and Mn provide additional information for identifying metal oxides or clay minerals with unique elemental features, such as the iron-bearing minerals in brown to reddish colour. The dissolved anions Cl^- and SO_4^{2-} confirm the occurrence of chloride and sulfate, for example, $CaSO_4$ causes more hydration resulting from sulfate swelling (Butscher et al. 2016) and initiates secondary swelling. Results from this study are denoted in red, suggesting that groundwater from the study area contains relatively high sodium content, 191 mg/L, which favours the presence of Na-montmorillonite with greater swelling potential in the field. The impact of SO_4^{2-} would be less detrimental due to limited gypsum precipitation with low Ca concentration.

Identifying the solute dissolved in groundwater benefits the swelling prediction and associated control measures. Geochemical assessment indicates groundwater only contains ion concentrations one to two orders of magnitude lower than those in salt solutions used for treatment. In practice, groundwater chemistry may have limited effects and is demanding to quantify due to its compositional heterogeneity and variability. Nevertheless, the chemical considerations still warrant attention, particularly in a saline environment with high sodium content. Both earlier research (Savage 2005) and this study revealed that Na is one of the most critical factors participating in swelling, potentially affecting the implementation and maintenance of control measures. Therefore, groundwater chemistry assessment is recommended for the stability analysis for excavations in swelling rocks. Incorporating appropriate chemical treatment would be better to assess and manage swelling-induced floor heave.

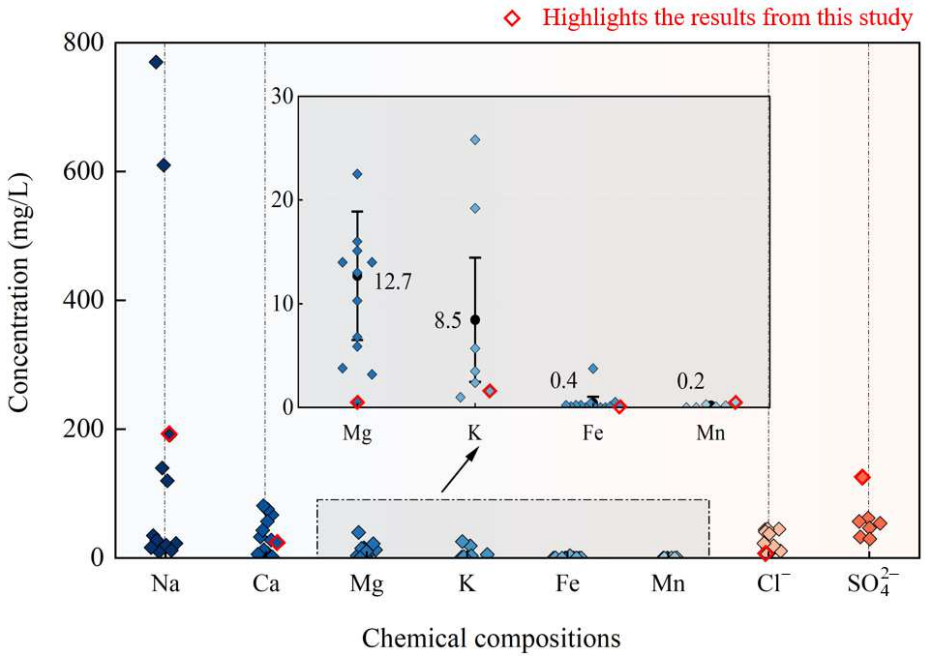


Fig. 17 Groundwater chemical compositions obtained from this study, Shultz (1988) and Whittall (1990).

6. Conclusion

In conclusion, this study investigates the swelling behaviour of geomaterials under different chemical treatments. Immersion tests are first conducted on compacted clays, considering the effects of cation type and concentration. At 1 M concentration, the KCl solution exhibits the most pronounced mitigation effects compared to $CaCl_2$ and NaCl. However, under a dilute concentration of 0.1 M, all saline solutions marginally promote clay swelling, with the performance ranked as NaCl > KCl > $CaCl_2$. This contrast is governed by osmotic pressure resulting from the Donnan equilibrium and limited double-layer compression during cation exchange Spraying is applied as a treatment method during wetting and drying cycles on clay specimens to evaluate the impact of KCl-based treatment. Repeated wetting and drying exacerbate the formation and propagation of surface cracking, whereas spraying KCl reduces the water absorption of the clay during re-saturation. Enhanced ventilation conditions can further improve the effectiveness of KCl treatment. In comparison, the clay specimen is highly saturated at the surface in DI water due to substantial water uptake.

Based on test results from compacted clays, KCl is applied to stabilise the swelling of intact rock specimens. The swelling potential, particularly osmotic swelling, of intact rocks is substantially less than that of clays prepared in the laboratory, as the rock matrix is strengthened by strong interparticle bonding resulting from cementation and other diagenesis processes. The expansion behaviour of tuff rocks is dominated by intra-crystalline swelling due to suppressed osmotic swelling. Microscopic analyses are conducted on rocks before and after treatment. SEM scans reveal that swelling alters the surface morphography of the rock, which is quantified by surface roughness parameters. Supported by EDS mapping, elemental abundances focus on high-contrast regions in SEM images, with illustrations in the z-axis of the 3D intensity plot. The spatial distributions of key elements identify a high colocalisation of K and Cl on the rock after treatment, corresponding to bright regions in SEM images. K and Cl are less detectable in the rock after immersion in DI water, implying that KCl precipitations are primarily sourced from the added chemical. However, the water evaporation due to oven-drying before scanning also contributes to the formation of salt crystals. Future studies will consider the use of Micro-CT to enhance microscopic observation of rock swelling under chemical effects.

The application of chemical treatment is also evaluated. KCl-based treatment is innovatively used to mitigate swelling of tuffaceous claystone. The tested rock after treatment is expected to be more durable against slaking and weathering in the field. Geochemical assessment of groundwater is recommended to account for saline conditions, such as elevated sodium concentrations, that may exacerbate swelling. Further research is required to implement and optimise chemical treatments for controlling swelling in field conditions.

Author Contributions

Wanqi Zhang: Formal analysis, Writing - Original Draft. Chengguo Zhang: Methodology, Writing - Review & Editing, Supervision. Honghao Chen: Methodology, Writing - Review & Editing. Joung Oh: Methodology, Supervision. Ismet Canbulat: Methodology, Supervision. Serkan Saydam: Methodology, Supervision, Project administration.

Statement and Declarations

Competing Interests: The authors declare that they have no known competing financial interests or personal relationships that could have appeared to influence the work reported in this paper.

652 **Reference**

653 Alaoui HM, Zhao C, Niu W, Wu D, Hicher P-Y (2025) Swelling pressure of clayey geomaterials: A comprehensive
654 analysis of experimental methods, numerical estimates and molecular dynamics simulations. Applied Clay
655 Science 276:107881. https://doi.org/10.1016/j.clay.2025.107881

656 Altmann S, Tournassat C, Goutelard F, Parneix J, Gimmi T, Maes N (2012) Diffusion-driven transport in clayrock
657 formations. Applied Geochemistry 27(2):463-478. https://doi.org/10.1016/j.apgeochem.2011.09.015

658 Alzamel M, Fall M, Haruna S (2022) Swelling ability and behaviour of bentonite-based materials for deep
659 repository engineered barrier systems: Influence of physical, chemical and thermal factors. Journal of Rock
660 Mechanics and Geotechnical Engineering 14(3):689-702. https://doi.org/10.1016/j.jrmge.2021.11.009

661 ASTM (2021) ASTM D4546-21: Standard Test Methods for One-Dimensional Swell or Collapse of Cohesive
662 Soils.

663 Barakat Y, Mokni N, Cui Y, Bernier F (2024) Effects of salinity and alkalinity on the volumetric deformation of
664 the Opalinus Clay from the Lower Sandy Facies (LSF) of Mont Terri Site. Rock Mechanics and Rock Engineering
665 57(11):1-23. https://doi.org/10.1007/s00603-024-04028-9

666 Barman D, Dash SK (2022) Stabilization of expansive soils using chemical additives: A review. Journal of Rock
667 Mechanics and Geotechnical Engineering 14(4):1319-1342. https://doi.org/10.1016/j.jrmge.2022.02.011

668 Bilir ME, Sarıgül G (2021) Stability assessment of Terzili tunnel in swelling rock mass. Arabian Journal of
669 Geosciences 14(11):965. https://doi.org/10.1007/s12517-021-07325-7

670 Butscher C, Mutschler T, Blum P (2016) Swelling of clay-sulfate rocks: A review of processes and controls. Rock
671 Mechanics and Rock Engineering 49:1533-1549. https://doi.org/10.1007/s00603-015-0827-6

672 Chai Z, Kang T, Feng G (2014) Effect of aqueous solution chemistry on the swelling of clayey rock. Applied Clay
673 Science 93:12-16. https://doi.org/10.1016/j.clay.2014.02.027

674 Chen M, Zhang C, Canbulat I, Saydam S (2025) Assessment of groundwater depressurisation due to mining
675 considering flow nonlinearity in connected fractures. Rock Mechanics and Rock Engineering 58(4):4347-4376.
676 https://doi.org/10.1007/s00603-025-04434-7

677 David K (2018) Groundwater changes in a sedimentary sequence associated with underground mining-A
678 multidisciplinary approach. Dissertation, University of New South Wales, Sydney, Australia.

679 Doostmohammadi R, Moosavi M, Mutschler T, Osan C (2009) Influence of cyclic wetting and drying on swelling
680 behavior of mudstone in south west of Iran. Environmental Geology 58(5):999-1009.
681 https://doi.org/10.1007/s00254-008-1579-3

682 Duncan N, Dunne M, Petty S (1968) Swelling characteristics of rock. Water Power 20(5):185-192.

683 Galvin J, Hebblewhite B, Vasundhara (1999 of Conference) Geomechanics developments in mining coal under
684 strong roof and weak floor conditions.9th ISRM Congress pp 277-281.

685 Gao Q, Yu H, Zeng L, Huang Y (2023) Characterization of water retention behavior of cracked compacted lateritic
686 soil exposed to wet-dry cycles. Bulletin of Engineering Geology and the Environment 82(2):61.
687 https://doi.org/10.1007/s10064-023-03089-4

688 Ghorbani M, Shahriar K, Sharifzadeh M, Masoudi R (2020) A critical review on the developments of rock support
689 systems in high stress ground conditions. International Journal of Mining Science and Technology 30(5):555-572.
690 https://doi.org/10.1016/j.ijmst.2020.06.002

691 Guan H, Ren Y, Ling S, Wu X, Yu T, Li X, Wang S, Sun C (2024) Microstructure and water-swelling mechanism
692 of red-bed mudstone in the Xining region, Northeastern Tibetan Plateau. Journal of Rock Mechanics and
693 Geotechnical Engineering 16(7):2537-2551. https://doi.org/10.1016/j.jrmge.2023.11.031

He B, Ding S, Shi Z (2021) A comparison between profile and areal surface roughness parameters. Metrology and Measurement Systems 28(3):413-438. https://10.24425/mms.2021.137133

Hebblewhite B, Galvin J, Sainsbury B-A, Vasundhara, Gale W, Whiteley R, Hill D (2005) ACARP Project C9018: Systems Approach to Pillar Design. Australian Coal Industry's Research Program

Hosseinzadeh N, Montanari L, Suraneni P (2022) Durability of concretes exposed to high concentrations of CaCl2 and MgCl2. Materials and Structures 55(6):153. https://doi.org/10.1617/s11527-022-01992-y

ISRM (1979) Suggest methods for determining water content, porosity, density, absorption and related properties and swelling and slake-durability index properties. International Journal of Rock Mechanics and Mining Sciences & Geomechanics Abstracts 16(2):143-151. https://doi.org/10.1016/0148-9062(79)91452-9

ISRM (1999) Suggested methods for laboratory testing of swelling rocks. International Journal of Rock Mechanics and Mining Sciences 36(3):291-306. https://doi.org/10.1016/S0148-9062(99)00005-4

Jiang S, Huang M, Jiang Y, Xu C, Li B (2022) NMR-based investigation on the wet–dry deterioration characteristics of gypsiferous rocks surrounding underground excavations. Rock Mechanics and Rock Engineering 55(4):2323-2339. https://doi.org/10.1007/s00603-022-02780-4

Karami M, Sedaee B, Nakhaee A (2023) Effect of different injection fluids scenarios on swelling and migration of common clays in case of permeability variations: a micromodel study. Journal of Petroleum Exploration and Production Technology 13(8):1761-1787. https://doi.org/10.1007/s13202-023-01628-z

Li L, Liu H (2013) A numerical study of the mechanical response to excavation and ventilation around tunnels in clay rocks. International Journal of Rock Mechanics and Mining Sciences 59:22-32. https://doi.org/10.1016/j.ijrmms.2012.11.005

Li X, Liu X, Tan Y, Chen A, Wang H, Wang X, Yang S (2023) Rheological mechanical properties and its constitutive relation of soft rock considering influence of clay mineral composition and content. International Journal of Coal Science & Technology 10(1):48. https://doi.org/10.1007/s40789-023-00615-3

Liu L, Chen Y, Ye W, Cui Y, Wu D (2018) Effects of hyperalkaline solutions on the swelling pressure of compacted Gaomiaozi (GMZ) bentonite from the viewpoint of Na+ cations and OH–anions. Applied Clay Science 161:334-342. https://doi.org/10.1016/j.clay.2018.04.023

Ma J, Chen Y, Jia L, Ye W, Wu D, Wang Q (2024) Anisotropic swelling pressures of compacted GMZ bentonite infiltrated with salt solutions. Journal of Rock Mechanics and Geotechnical Engineering https://doi.org/10.1016/j.jrmge.2024.01.024

Madsen FT, Müller-Vonmoos M (1989) The swelling behaviour of clays. Applied Clay Science 4(2):143-156. https://doi.org/10.1016/0169-1317(89)90005-7

Mayor JC, Velasco M, García Siñeriz JL (2007) Ventilation experiment in the Mont Terri underground laboratory. Physics and Chemistry of the Earth, Parts A/B/C 32(8-14):616-628. https://doi.org/10.1016/j.pce.2006.04.030

McNally G, Branagan D (2014) Geotechnical consequences of the Newcastle Coal Measures rocks. Australian Journal of Earth Sciences 61(3):363-374. https://doi.org/10.1080/08120099.2013.841753

Mehdizad A, Pourafshary P, Sedaee B (2022) Visual investigation of simultaneous clay swelling and migration mechanisms and formation damage consequences using micromodels. Journal of Petroleum Science and Engineering 214:110561. https://doi.org/10.1016/j.petrol.2022.110561

Middelhoff M, Cuisinier O, Masrouri F, Talandier J, Conil N (2020) Combined impact of selected material properties and environmental conditions on the swelling pressure of compacted claystone/bentonite mixtures. Applied Clay Science 184:105389. https://doi.org/10.1016/j.clay.2019.105389

Mo S, Ramandi HL, Oh J, Masoumi H, Canbulat I, Hebblewhite B, Saydam S (2020) A new coal mine floor rating system and its application to assess the potential of floor heave. International Journal of Rock Mechanics and Mining Sciences 128:104241. https://doi.org/10.1016/j.ijrmms.2020.104241

Morkel J, Saydam S (2008) The influence of potassium on the weathering properties of kimberlite and the information provided by different testing methods. International Journal of Rock Mechanics and Mining Sciences 45(7):1187-1194. https://doi.org/10.1016/j.ijrmms.2008.01.011

Murtaza M, Allowaim MA, Syed NA, Mahmoud M, Kamal MS, Rana A (2025) Effectiveness of Chloride Salts in Shale Swelling Inhibition: An Assessment of Its Impact on Drilling Fluid Performance. Arabian Journal for Science and Engineering:1-14. https://doi.org/10.1007/s13369-024-09857-y

Nemcik JA (2003) Floor failure mechanisms at underground longwall face.

Nunt-Jaruwong S (2006) Engineering geology of the Patonga Claystone, Central Coast, New South Wales, with particular reference to slaking behaviour. Dissertation, UNSW Sydney.

Olivier HJ (1979) A new engineering-geological rock durability classification. Engineering Geology 14(4):255-279. https://doi.org/10.1016/0013-7952(79)90067-X

Pejon OJ, Zuquette LV (2002) Analysis of cyclic swelling of mudrocks. Engineering Geology 67(1-2):97-108. https://doi.org/10.1016/S0013-7952(02)00147-3

Pimentel E (2015) Existing methods for swelling tests–a critical review. Energy Procedia 76:96-105. https://doi.org/10.1016/j.egypro.2015.07.857

Pusch R, Yong RN (2006) Microstructure of smectite clays and engineering performance. CRC Press

Rastegarnia A, Lashkaripour GR, Sharifi Teshnizi E, Ghafoori M (2021) Evaluation of engineering characteristics and estimation of static properties of clay-bearing rocks. Environmental Earth Sciences 80:1-24.

Rosentritt M, Schneider Feyrer S, Kurzendorfer L (2024) Comparison of surface roughness parameters Ra/Sa and Rz/Sz with different measuring devices. Journal of the Mechanical Behavior of Biomedical Materials 150:106349. https://doi.org/10.1016/j.jmbbm.2023.106349

Savage D (2005) The effects of high salinity groundwater on the performance of clay barriers.

Seedsman RW (1988) Roof and floor instability with the Awaba Tuff. Proceedings of the Twenty-Second Symposium on Advances in the Study of the Sydney Basin, Newcastle, New South Wales, Australia, pp 79-82.

Shehata A, Fall M, Detellier C, Alzamel M (2021) Effect of groundwater chemistry and temperature on swelling and microstructural properties of sand–bentonite for barriers of radioactive waste repositories. Bulletin of Engineering Geology and the Environment 80(2):1857-1873. https://doi.org/10.1007/s10064-020-02020-5

Shultz RA (1988) Ground-water hydrology of Marshall County, West Virginia, with emphasis on the effects of longwall coal mining. US Geological Survey

Sridharan A, Jayadeva M (1982) Double layer theory and compressibility of clays. Geotechnique 32(2):133-144. https://doi.org/10.1680/geot.1982.32.2.133

Steiner W, Schwalt M (2019) In-situ swelling pressures in sulphate bearing rocks: Findings from field observations. Proceedings of 14th ISRM Congress, Foz do Iguaçu, Brazil, pp 1724-1731.

Tang C, Cui Y, Shi B, Tang A, Liu C (2011) Desiccation and cracking behaviour of clay layer from slurry state under wetting–drying cycles. Geoderma 166(1):111-118. https://doi.org/10.1016/j.geoderma.2011.07.018

Vasundhara (1999) Engineered Mine Design in Soft Strata Environments: Geomechanical Behaviour of Soft Floor Strata in Underground Coal Mines: ACARP Project No. C4026 (End of Grant Report). Department of Mining Engineering, University of New South Wales

776 Vergara MR, Triantafyllidis T (2015) Swelling behavior of volcanic rocks under cyclic wetting and drying.
777 International Journal of Rock Mechanics and Mining Sciences 80:231-240.
778 https://doi.org/10.1016/j.ijrmms.2015.08.021

779 Wakim J, Hadj Hassen F, De Windt L (2009) Effect of aqueous solution chemistry on the swelling and shrinkage
780 of the Tournemire shale. International Journal of Rock Mechanics and Mining Sciences 46(8):1378-1382.
781 https://doi.org/10.1016/j.ijrmms.2009.08.002

782 Wang Q, Xu Y, Su W, Ye W, Chen Y, Lai H (2023) Enhancement mechanism of remolding on the swelling behavior
783 of expansive stiff clay: from microstructure perspective. Environmental Earth Sciences 82(16):378.
784 https://doi.org/10.1007/s12665-023-11071-2

785 Whittall PW (1990) Hydrogeological investigation and analysis of a major inundation at Kemira Colliery.
786 Dissertation, University of Wollongong.

787 Xiang G, Ye W, Xu Y, Jalal FE (2020) Swelling deformation of Na-bentonite in solutions containing different
788 cations. Engineering Geology 277:105757. https://doi.org/10.1016/j.enggeo.2020.105757

789 Yang X, Wang J, Zhu C, He M, Gao Y (2019) Effect of wetting and drying cycles on microstructure of rock based
790 on SEM. Environmental Earth Sciences 78(6):183. https://doi.org/10.1007/s12665-019-8191-6

791 Yunus NM, Wanatowski D, Stace L (2012) Effectiveness of chloride salts on the behaviour of lime-stabilised
792 organic clay. GEOMATE Journal 3(6):407-412.

793 Zhang F, Cui Y, Conil N, Talandier J (2020) Assessment of swelling pressure determination methods with intact
794 Callovo-Oxfordian claystone. Rock Mechanics and Rock Engineering 53:1879-1888.
795 https://doi.org/10.1007/s00603-019-02016-y

796 Zhang S, Zhu T, Zheng P, Ye L (2024) Evaluation and prediction of swelling properties of bentonite under the
797 action of salt solution. Applied Clay Science 258:107453. https://doi.org/10.1016/j.clay.2024.107453

798 Zhang W, Zhang C, Oh J, Canbulat I, Saydam S (2026) Numerical study on the hydro-mechanical behaviour of
799 swelling rocks in long-term floor stability. Rock Mechanics Bulletin:100349.
800 https://doi.org/10.1016/j.rockmb.2026.100349

801